The Journal of Chemical Physics ARTICLE scitation.org/journal/jcp

Discrete stochastic models of SELEX: Aptamer capture probabilities and protocol optimization

Cite as: J. Chem. Phys. 156, 244103 (2022); doi: 10.1063/5.0094307
Submitted: 2 April 2022 • Accepted: 2 June 2022 •
Published Online: 22 June 2022

Yue Wang,[1] Bhaven A. Mistry,[2] and Tom Chou[1,3,a)]

AFFILIATIONS

[1] Department of Computational Medicine, University of California, Los Angeles, California 90095-1766, USA
[2] Department of Mathematical Sciences, Claremont McKenna College, Claremont, California 91711, USA
[3] Department of Mathematics, University of California, Los Angeles, California 90095-1555, USA

[a)] **Author to whom correspondence should be addressed:** tomchou@ucla.edu

ABSTRACT

Antibodies are important biomolecules that are often designed to recognize target antigens. However, they are expensive to produce and their relatively large size prevents their transport across lipid membranes. An alternative to antibodies is aptamers, short (~15 – 60 bp) oligonucleotides (and amino acid sequences) with specific secondary and tertiary structures that govern their affinity to specific target molecules. Aptamers are typically generated via solid phase oligonucleotide synthesis before selection and amplification through Systematic Evolution of Ligands by EXponential enrichment (SELEX), a process based on competitive binding that enriches the population of certain strands while removing unwanted sequences, yielding aptamers with high specificity and affinity to a target molecule. Mathematical analyses of SELEX have been formulated in the mass action limit, which assumes large system sizes and/or high aptamer and target molecule concentrations. In this paper, we develop a fully discrete stochastic model of SELEX. While converging to a mass-action model in the large system-size limit, our stochastic model allows us to study statistical quantities when the system size is small, such as the probability of losing the best-binding aptamer during each round of selection. Specifically, we find that optimal SELEX protocols in the stochastic model differ from those predicted by a deterministic model.

I. INTRODUCTION

A common goal in biophysics is precise targeting and isolation of biological molecules. In mammalian immune systems, antibodies are produced with variable regions in their peptide chain sequences to allow for a subset of them to strongly binding to a specific epitope, a binding site expressed on antigens or pathogenic molecules.[1–3] This feature of antibodies allows them to be used to deliver drugs to specific cancer cells, to mark the presence of certain proteins with immunofluorescence, or to inhibit viral entry of HIV-1 into their host cells.[4–6] The rapid increase of infectious diseases and viral outbreaks in recent years, such as Ebola, Zika, and coronavirus, has also led to high demand for laboratory-made monoclonal antibodies to be used in diagnostic/therapeutic contexts. However, monoclonal antibodies are costly to produce and the protocols involved are time-consuming.[7–9]

A more modern alternative to molecular targeting using antibodies is based on the use of aptamers, short DNA or RNA oligonucleotides, usually about 15–60 bases in length.[10] More recent approaches have also combined nucleotide bases with polypeptides. Aptamers may fold into a sequence-dependent conformation that can result in them performing specific enzymatic functions or exhibiting binding affinities to certain epitopes. The specific binding affinities to targets can be comparable to those of antibodies, though the smaller aptamer sizes allow for easier transport through lipid membranes for intracellular marking. More importantly, the synthesis of aptamers can be much simpler than that of antibodies since the nucleotide sequences are chemically synthesized. Since *ab initio* oligonucleotide design is difficult, the different oligonucleotide sequences are usually combined to form a library of aptamers. The desired sequence is then isolated and amplified by a selection process known as systematic evolution of ligands by exponential enrichment (SELEX).[10–12]

The goal of a SELEX protocol is to identify and isolate the aptamer sequence that binds a specified target molecule with the highest affinity. The process of SELEX begins with a solution

(library) containing many different aptamer sequences. The aptamer library may contain structurally close sequences that bind the target almost as well as the strongest binder. In order to filter out the weaker-binding aptamers and obtain a solution of only the desired strongly binding aptamers, a solution of target molecules is added to the entire aptamer solution. After mixing and equilibration, unbound aptamers are removed and the remaining aptamer-target complexes are isolated. These complexes are then dissociated in solution, and the corresponding aptamers are amplified via the polymerase chain reaction (PCR). After one cycle of SELEX, these aptamers are then exposed to the same target again to successively prune weaker binders and isolate the strongest ones. Komarova and Kuznetsov[13] provide more detailed, biochemical descriptions of SELEX and discuss, qualitatively, factors to consider in optimizing specific stages.

One expects that after each round of target exposure and PCR, the multi-sequence aptamer solution becomes more concentrated in those aptamers with a stronger affinity to the target. However, in the early rounds, when there might be a large number of different aptamers in the solution, the number of strongest binders may be small, necessitating a statistical/stochastic description. From round to round, one can use different numbers of target molecules, but the relative abundances of different aptamer types are fixed by the previous round. Target and aptamer concentrations can determine the abundance and likelihood of capturing the highest affinity aptamer. A SELEX protocol or "policy" describes how to assign such concentrations in each round.[14] Different policies are expected to lead to different relative abundances of different aptamer types as they evolve over multiple rounds of SELEX.

Previous mathematical models have been developed to quantify SELEX. Most of the models assume that the number of targets and aptamers is large enough so that the law of mass action applies and the binding/unbinding kinetics are deterministic.[11,12,15,16] Wang *et al.* concluded that within the mass-action limit, low concentrations of the target are ideal for capturing the best-binding aptamer with the fewest rounds of SELEX.[11] However, at low target concentrations, competition among the aptamer species for limited binding sites will increase the probability that not even a single target molecule captures the strongest binding aptamer, forever losing the desired aptamer. Thus, the statistics of the pattern of aptamers captured in each round of SELEX will depend on the distribution of binding rates and energies associated with the aptamer library, as well as the abundances of aptamers and targets. Low abundances lead to larger relative number fluctuations that affect aptamer abundances for subsequent rounds.

Kinetic descriptions based on the mass-action law have been adapted to incorporate stochastic small number effects.[14,17] Aita *et al.*[17] first developed a hybrid model and assumed Gaussian distribution of binding energies, while Spill *et al.*[14] merged mass-action descriptions with approximate stochastic descriptions and Monte Carlo simulations to show how low copy number high affinity aptamers contribute to uncertainty in selection outcomes.

Here, we formally develop a fully stochastic model of SELEX that considers discrete numbers of all molecules, including all aptamer types. To focus statistical properties of one specific aptamer type (e.g., the best binder), we self-consistently lump all other aptamer types into one effective pool. Then, we determine the upper and lower bounds for the proportion of the best aptamer after one round of SELEX. Our results suggest optimal policies that maximize the expected proportion of the strongest binding aptamer after multiple rounds of SELEX, as well as the probability of loss of the strongest binder. We find distinctly different optimal policies depending on whether mass-action kinetics or a discrete stochastic/combinatorial model was used.

II. BACKGROUND AND SETUP

A. Markov chain

One way to formulate a discrete-state stochastic model is to start from a continuous-time Markov chain connecting system configurations, or states.[14] At any specific time, each of these states can represent a system with specific numbers of bound and unbound aptamers. Transitions from state i to state j occur with non-negative transition rates $r_{i\to j} \geq 0$. We will always assume this Markov chain is commutative, meaning that starting from any state i, we can jump to any state j in a finite number of steps. Then, as time $t \to \infty$, the probability that the process X is in state i, $\mathbb{P}(X = i)$, converges to the unique stationary probability distribution $\mathbb{P}_i$, which only depends on the transition rates.

Now, further consider a cycle of events in this Markov chain, described by the sequence of states $i \to j \to k \to i$. If we have $r_{i\to j}r_{j\to k}r_{k\to i} = r_{j\to i}r_{k\to j}r_{i\to k}$, then we call this cycle "symmetric." If all cycles in this Markov chain are symmetric, then this Markov chain satisfies *detailed balance*.[18] In fact, we need not check that all cycles are symmetric, but only the "elementary" ones[19] since more complicated cycles can be decomposed into combinations of elementary cycles. Specifically, if a Markov chain has no cycle (e.g., a random walk on all integers $\mathbb{Z}$), then it naturally satisfies detailed balance. If the Markov chain satisfies detailed balance, then the stationary distribution satisfies $r_{i\to j}\mathbb{P}_i = r_{j\to i}\mathbb{P}_j$. These detailed balance relationships provide a convenient way to calculate stationary distributions and is equivalent to using classical statistical mechanical approaches that use free energy differences and the Boltzmann distribution.

B. Stationary distribution

Since the chemical binding and unbinding events between target and aptamer molecules are intrinsically stochastic, we build a continuous-time Markov chain model to describe them and calculate the stationary distribution. Assume we have one type of target molecule, S, and M types of aptamer molecules, A_i, $1 \leq i \leq M$. Each type of aptamer can participate in the binding reaction $\mathrm{A}_i + \mathrm{S} \rightleftharpoons \mathrm{A}_i\mathrm{S}$. The activation energy for $\mathrm{A}_i + \mathrm{S} \to \mathrm{A}_i\mathrm{S}$ is defined as G_i^+ while that for $\mathrm{A}_i\mathrm{S} \to \mathrm{A}_i + \mathrm{S}$ is denoted G_i^-. Different types of aptamers i can have different activation energies $G_i^\pm$. For each target molecule, we define a small "dimerization volume" v surrounding itself within which an aptamer molecule may be present. Only if an aptamer molecule is within this contact volume can it form a bond with (bind to) the target molecule.

First consider a system with a single A_i molecule and S_T target molecules within a fixed system volume V. As shown in Fig. 1, this aptamer molecule can be in one of three states: (i) not within the dimerization volume of any target, denoted as $(1, 0, 0)$; (ii) within the dimerization volume of one target (associated), but not bound, denoted as $(0, 1, 0)$; and (iii) bound to a target, denoted as $(0, 0, 1)$.

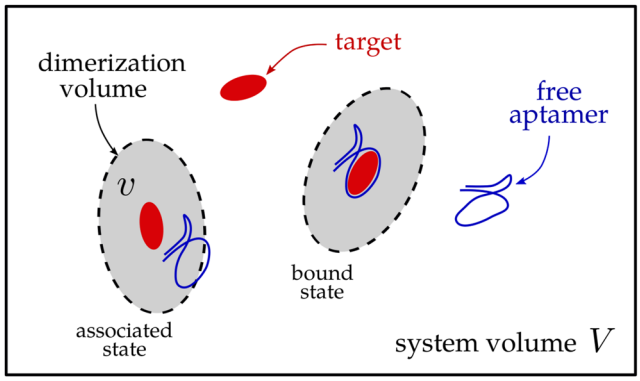

FIG. 1. Multiple targets and a single aptamer type in a system volume V. Each target is surrounded by an interaction volume v, which is roughly the average of the target and aptamer molecular volumes. Each target can either be associated with an aptamer or bound to one (one-to-one stoichiometry, associated, or bound). Only if the aptamer is within this v volume, it can bind to this target.

The transition between $(1,0,0)$ and $(0,1,0)$ occurs via free diffusion. Thus, the transition rates satisfy

$$\frac{r[(1,0,0)\to(0,1,0)]}{r[(0,1,0)\to(1,0,0)]} = \frac{S_T v}{V - S_T v}, \tag{1}$$

since the total dimerization volume is $S_T v$, and the "free" volume is $V - S_T v$. The transition between $(0,1,0)$ and $(0,0,1)$ represents aptamer-target binding (dimerization) and unbinding. If we define the activation energies by $r[(0,1,0)\to(0,0,1)] \propto e^{-\beta G_i^+}$ and $r[(0,0,1)\to(0,1,0)] \propto e^{-\beta G_i^-}$ ($\beta = (k_B T)^{-1}$), with the same proportionality,

$$\frac{r[(0,1,0)\to(0,0,1)]}{r[(0,0,1)\to(0,1,0)]} = e^{-\beta\Delta G_i}, \tag{2}$$

where $\Delta G_i \equiv G_i^+ - G_i^-$. For detailed discussions about binding probability and thermodynamics, readers may refer to papers by Atherton *et al.* and de Jong *et al.*[20,21] This three-state Markov chain has no cycle [state $(1,0,0)$ and $(0,0,1)$ are not connected], meaning that it satisfies detailed balance. Thus, upon imposing the detailed balancing conditions $r_{i\to j}\mathbb{P}_i = r_{j\to i}\mathbb{P}_j$, we have for this simple system $\mathbb{P}(0,1,0)/\mathbb{P}(1,0,0) = S_T v/(V - S_T v)$ and $\mathbb{P}(0,0,1)/\mathbb{P}(0,1,0) = e^{-\beta\Delta G_i}$. Normalization $\mathbb{P}(0,0,1) + \mathbb{P}(0,1,0) + \mathbb{P}(1,0,0) = 1$ provides the final condition leading to the solution

$$\begin{aligned}
\mathbb{P}(1,0,0) &= \frac{V - S_T v}{V + S_T v e^{-\beta\Delta G_i}},\\
\mathbb{P}(0,1,0) &= \frac{S_T v}{V + S_T v e^{-\beta\Delta G_i}},\\
\mathbb{P}(0,0,1) &= \frac{S_T v e^{-\beta\Delta G_i}}{V + S_T v e^{-\beta\Delta G_i}}.
\end{aligned} \tag{3}$$

Since we only focus on whether or not aptamers are bound, and not on their locations, we can combine the two unbound states $(1,0,0)$ and $(0,1,0)$ into one unbound state to obtain an effective two-state Markov chain. The ratio of bound to unbound probabilities is thus

$$\frac{\mathbb{P}(\text{bound})}{\mathbb{P}(\text{unbound})} = \frac{S_T v}{V} e^{-\beta\Delta G_i} \equiv S_T \bar{K}_i, \tag{4}$$

where we define the dimensionless association coefficient of type i aptamer $\bar{K}_i \equiv (v/V)\exp(-\beta\Delta G_i)$. Here, $S_T\bar{K}_i$ is the ratio of transition rates between two states. Table I lists the variables and parameters used to construct and analyze our model. Note the underlying *association constant* $K_i = v e^{-\beta\Delta G_i}$ carries units of per concentration, inverse of a second order dissociation constant.

We now extend the setup described above to include multiple aptamer types A_i, with A_i of each type in the system volume V. As in the discussion above, we combine states that differ only by aptamer location and just consider whether aptamers are bound to targets. Given the aptamer populations $\{A_1, A_2, \ldots, A_M\}$ and the total number of target molecules S_T, the system state can be described by the numbers of aptamers bound to target molecules $\mathbf{a} \equiv (a_1, a_2, \ldots, a_M)$. If the current state is $\mathbf{a}$, the rate of having one more bound A_i is proportional to $\bar{s}\bar{a}_i\bar{K}_i$, where $\bar{s} = S_T - s$ is the number of unbound targets and $\bar{a}_i = A_i - a_i$ is the number of unbound A_i aptamers. If the current state is $(a_1, \ldots, a_i + 1, \ldots, a_M)$, the dissociation rate into state $\mathbf{a}$ is proportional to $a_i + 1$, the number of bound A_i aptamers. In Subsection 2 of the Appendix, we show the relationship between transition rates,

$$\frac{r[\mathbf{a}\to(a_1,\ldots,a_i+1,\ldots,a_M)]}{r[(a_1,\ldots,a_i+1,\ldots,a_M)\to\mathbf{a}]} = \frac{\bar{a}_i\bar{s}}{a_i+1}\bar{K}_i. \tag{5}$$

We can verify that this process satisfies detailed balance so that

$$\begin{aligned}
\frac{\mathbb{P}(a_1,\ldots,a_i+1,\ldots,a_M)}{\mathbb{P}(\mathbf{a})} &= \frac{r[\mathbf{a}\to(a_1,\ldots,a_i+1,\ldots,a_M)]}{r[(a_1,\ldots,a_i+1,\ldots,a_M)\to\mathbf{a}]}\\
&= \frac{\bar{a}_i\bar{s}}{a_i+1}\bar{K}_i.
\end{aligned} \tag{6}$$

Thus, the stationary probability distribution satisfies

$$\begin{aligned}
\mathbb{P}(\mathbf{a}) &= \mathbb{P}(0,a_2,\ldots,a_M)\frac{S_T!}{(S_T-a_1)!}\frac{A_1!\,\bar{K}_1^{a_1}}{(A_1-a_1)!\,a_1!}\\
&= \mathbb{P}(0,0,a_3,\ldots,a_M)\frac{S_T!}{(S_T-a_1-a_2)!}\\
&\quad\times\frac{A_1!\,\bar{K}_1^{a_1}}{(A_1-a_1)!\,a_1!}\frac{A_2!\,\bar{K}_2^{a_2}}{(A_2-a_2)!\,a_2!}\\
&\quad\vdots\\
&= \mathbb{P}(0,\ldots,0)\frac{S_T!}{(S_T-a_s)!}\prod_{i=1}^{M}\frac{A_i!\,\bar{K}_i^{a_i}}{(A_i-a_i)!\,a_i!}\\
&= \mathbb{P}(0,\ldots,0)\binom{S_T}{S_T-a_s,a_1,\ldots,a_M}\\
&\quad\times\left[\prod_{i=1}^{M}\binom{A_i}{a_i}\right]\times\left[\prod_{i=1}^{M}a_i!\right]\times\left[\prod_{i=1}^{M}\bar{K}_i^{a_i}\right],
\end{aligned} \tag{7}$$

where $a_s \equiv \sum_{i=1}^{M} a_i$ is the total number of bound aptamers. The second term in the last line of Eq. (7) is the number of ways S_T targets can be distributed out to the M species and unbound state; the third

TABLE I. Relevant variables and parameters for our discrete stochastic SELEX model.

Symbol	Quantity	Relationships	Typical values
M	Total no. of aptamer types (richness)	$\cdots$	10^3–10^{14}
A_i	Total aptamers molecules of type i	$\cdots$	1–10^{10}
A_{T}	Total no. of aptamers	$A_{\mathrm{T}} = \sum_{i=1}^{M} A_i$	10^4–10^{15}
a_i	No. of bound type-i aptamers	$\cdots$	1–10^{10}
$\bar{a}_i$	No. of unbound type-i aptamers	$\bar{a}_i = A_i - a_i$	1–10^{10}
a_{s}	Total no. of bound aptamers	$a_{\mathrm{s}} = \sum_{i=1}^{M} a_i$	10^2–10^{13}
S_{T}	Total no. of target molecules	$\cdots$	10^3–10^{15}
s	Total no. of bound targets	$s = a_{\mathrm{s}}$	10^2–10^{13}
$\bar{s}$	Total no. of unbound targets	$S_{\mathrm{T}} = s + \bar{s}$	10^3–10^{15}
V	Total system volume	$\cdots$	1–10^4 μl
v	Molecular dimerization volume	$\cdots$	10^{-18} – 10^{-12} μl
ΔG_i	Energy of target-aptamer i binding	$\Delta G_i = G_i^+ - G_i^-$	1–25$k_{\mathrm{B}}T$
K_i	Aptamer i per particle association constant	$K_i = ve^{-\beta \Delta G_i}$	10^{-8}–10^{-4} μl
$\tilde{K}_i$	Aptamer i per volume association coefficient	$\tilde{K}_i = K_i/V$	10^{-12}–10^{-4}

term is the number of ways one can choose the a_i bound aptamers from the A_i possible options, for all i species; the fourth term is the number of ways targets and aptamers of each species fated for binding can be paired; the last term is the relative probability weight for bound aptamers. The product of the second, third, and fourth terms represents the number of configurations that in a system with S_{T} distinguishable targets, a_i targets are chosen to pair with a_i aptamers of type A_i, which themselves are chosen from A_i distinguishable A_i aptamers.

Then, for the set of states,

$$\mathcal{S} \equiv \{(a_1, \ldots, a_M) | 0 \le a_i \le A_i \text{ for each } i,\ a_{\mathrm{s}} \le S_{\mathrm{T}}\},$$

we use the normalization condition $\sum_{\mathbf{a} \in \mathcal{S}} \mathbb{P}(\mathbf{a}) = 1$ to determine $\mathbb{P}(0, \ldots, 0)$ and define the partition function $Z \equiv 1/\mathbb{P}(0, \ldots, 0)$,

$$Z = \sum_{\mathbf{a} \in \mathcal{S}} \frac{S_{\mathrm{T}}!}{(S_{\mathrm{T}} - a_{\mathrm{s}})!} \prod_{i=1}^{M} \frac{A_i!\, \tilde{K}_i^{a_i}}{(A_i - a_i)!\, a_i!}. \tag{8}$$

The equilibrium probability of being in a state $\mathbf{a}$ is then given explicitly by Eq. (7), which contains the usual Boltzmann factors over the binding energies embedded in the $\tilde{K}_i$ terms.

III. MASS ACTION LIMIT

The stationary distribution reaches a maximum if

$$\frac{\bar{s}\bar{a}_i}{a_i + 1} \tilde{K}_i = \frac{(\bar{s}/V)(\bar{a}_i/V)}{(a_i + 1)/V} v e^{-\beta \Delta G_i} = 1 \tag{9}$$

for each i. For $a_i \gg 1$, constraint is equivalent to Refs. 11 and 22,

$$\frac{[a_i]}{[\bar{s}][\bar{a}_i]} = K_i \Rightarrow [a_i] = \frac{[A_i] K_i}{K_i + 1/[\bar{s}]}, \tag{10}$$

where $[\cdot]$ denotes concentrations. Since K_i is the association constant, $[\bar{s}]$ is the concentration of unbound target S, $[\bar{a}_i]$ is the concentration of unbound aptamer A_i, and $[a_i]$ is the concentration of bound aptamer A_i. Equation (10) is simply the mass action law, shown explicitly to be the large system size limit of the Markov chain model.

Assume that we order the labels of the aptamer species in a way such that here $K_1 \ge K_2 \ge \ldots \ge K_M$, i.e., type A_1 is the strongest binder. A useful quantity is the proportion of all bound aptamers that are of type A_1. In the mass-action limit, if we decrease $[S_{\mathrm{T}}]$ or increase $[A_{\mathrm{T}}]$ (keeping the proportions of $[A_i]$), the fraction of bound A_1 in all bound aptamers increases (proved in Subsection 3 of the Appendix). Therefore, to obtain the largest $[a_1]/[a_{\mathrm{s}}]$, we should take large $[A_{\mathrm{T}}]$ and small $[S_{\mathrm{T}}]$, rendering $[\bar{s}]$ small. In this case, $[a_i] \approx [A_i] K_i [\bar{s}]$, and $[a_1]/[a_{\mathrm{s}}]$ approaches the upper bound $[A_1]K_1/(\sum_{i=1}^{M} [A_i] K_i)$. When we take small $[A_{\mathrm{T}}]$ and large $[S_{\mathrm{T}}]$, $[\bar{s}]$ is also large. Then, $[a_i] \approx [A_i]$, and the fraction $[a_1]/[a_{\mathrm{s}}]$ approaches its lower bound $[A_1]/(\sum_{i=1}^{M} [A_i])$. This result has been noted by Rudzinski *et al.* in an unpublished report.

IV. APPROXIMATION OF THE DISCRETE MODEL

We have shown using the Markov chain model that the equilibrium distribution is

$$\mathbb{P}(a_1, \ldots, a_M) = \frac{S_{\mathrm{T}}!}{Z(S_{\mathrm{T}} - a_{\mathrm{s}})!} \prod_{i=1}^{M} \frac{A_i!\, \tilde{K}_i^{a_i}}{(A_i - a_i)!\, a_i!}. \tag{11}$$

One reason that this probability distribution is difficult to handle is because it requires calculation of the partition function Z. In this section, we consider two limits of Eq. (11), both of which use the approximation

$$\begin{aligned} \frac{a!}{(a-b)!} &= a(a-1)(a-2)\ldots(a-b+1) \\ &\approx a^b \left[1 + \mathcal{O}\left(b^2/a\right)\right] \end{aligned} \tag{12}$$

for $b^2/a \ll 1$.

A. Small S_T approximation

If $A_i \gg S_T^2$ for each i, since $a_i \le S_T$, each $A_i!/(A_i - a_i)!$ term can be approximated by $A_i^{a_i}$ to yield

$$\mathbb{P}(\mathbf{a}) = \frac{S_T!}{Z(S_T - a_s)!\prod_{i=1}^M a_i!}\prod_{i=1}^M (A_i\tilde{K}_i)^{a_i}. \tag{13}$$

Upon summing Eq. (13) over all $\mathbf{a}$ and comparing each term with the multinomial expansion of $(1 + \sum_{i=1}^M A_i\tilde{K}_i)^{S_T}$, we find $Z = (1 + \sum_{i=1}^M A_i\tilde{K}_i)^{S_T}$ and

$$\mathbb{P}(\mathbf{a}) = \frac{S_T!}{(S_T - a_s)!\prod_{i=1}^M a_i!}\, p_0^{S_T - a_s}\prod_{i=1}^M p_i^{a_i}, \tag{14}$$

where $p_0 = 1/(1 + \sum_{i=1}^M A_i\tilde{K}_i)$ and $p_i = A_i\tilde{K}_i/(1 + \sum_{i=1}^M A_i\tilde{K}_i)$. Under this approximation, $(S_T - a_s a_1, \ldots, a_M)$ satisfies a multinomial distribution, and the target molecules are independent. Each target has probability p_i of being bound to an A_i aptamer and probability p_0 to be unbound. Additional mathematical details are given in Subsection 4 of the Appendix.

To compute the expected proportion of bound aptamer A_j, we note that $(a_j/a_s)\mathbb{P}(\mathbf{a})$ can be expressed as

$$\begin{aligned}\frac{a_j}{a_s}\mathbb{P}(\mathbf{a}) &= \frac{a_j}{a_s}\binom{S_T}{a_s} p_0^{S_T - a_s}\frac{a_s!}{\prod_{i=1}^M a_i!}\prod_{i=1}^M p_i^{a_i},\\ &= \binom{S_T}{a_s} p_0^{S_T - a_s}\frac{p_j(a_s - 1)!p_j^{a_j - 1}}{(a_j - 1)!\prod_{i\neq j}^M a_i!}\prod_{i\neq j}^M p_i^{a_i},\end{aligned}$$

which is a multinomial expansion under a fixed sum $\sum_i^M a_i = a_s$. Summation over all possible $\mathbf{a}$ under this constraint gives

$$\begin{aligned}\sum_{a_1+\cdots a_M = a_s}\frac{a_j}{a_s}\mathbb{P}(\mathbf{a}) &= \binom{S_T}{a_s} p_0^{S_T - a_s} p_j\left(\sum_{i=1}^M p_i\right)^{a_s - 1}\\ &= \frac{p_j}{1 - p_0}\binom{S_T}{a_s} p_0^{S_T - a_s}(1 - p_0)^{a_s}.\end{aligned} \tag{15}$$

If we include only configurations $a_s \ge 1$ in calculating the expected fraction, we use $\mathbb{P}(\mathbf{a} \mid a_s \ge 1) = \mathbb{P}(\mathbf{a})/(1 - p_0^{S_T})$ in the final sum over $a_s \ge 1$ to find

$$\begin{aligned}\mathbb{E}\left[\frac{a_j}{a_s}\middle| a_s \ge 1\right] &= \sum_{a_s=1}^{S_T}\sum_{\sum_i^M a_i = a_s}\frac{a_j}{a_s}\mathbb{P}(\mathbf{a}|a_s \ge 1)\\ &= \frac{p_j}{1 - p_0} = \frac{A_j\tilde{K}_j}{\sum_{i=1}^M A_i\tilde{K}_i}.\end{aligned} \tag{16}$$

When $A_T \gg S_T^2$ and $S_T \gg 1/(1 - p_0)$, the probability $\mathbb{P}(a_s = 0) = p_0^{S_T}$ is negligible. Thus, the expected fraction of all bound aptamers that are the strongest binder A_1 approaches $A_1\tilde{K}_1/(\sum_{i=1}^M A_i\tilde{K}_i)$. We will show that this is the theoretical upper bound for the dimerized A_1 fraction. In fact, when $S_T \gg 1$, since different targets are independent, and by the law of large numbers, the proportion of bound A_1 (not just its expectation) converges to $A_1\tilde{K}_1/(\sum_{i=1}^M A_i\tilde{K}_i)$.

B. Large S_T approximation

If $S_T \gg A_T^2$, since $a_s \le A_T$, we can approximate $S_T!/(S_T - a_s)!$ in Eq. (11) by $S_T^{a_s}$. The equilibrium probability distribution takes on the product form

$$\mathbb{P}(\mathbf{a}) = \mathbb{P}(0, \ldots, 0)\prod_{i=1}^M \frac{A_i!\,(\tilde{K}_i S_T)^{a_i}}{(A_i - a_i)!\,a_i!}. \tag{17}$$

Since the number of targets is much larger than the number of aptamers, aptamers can bind independently and do not have to compete for free targets. For each aptamer type,

$$\mathbb{P}(a_i) = \mathbb{P}_i(0)\frac{A_i!\,(\tilde{K}_i S_T)^{a_i}}{(A_i - a_i)!\,a_i!}, \tag{18}$$

where normalization yields $\mathbb{P}_i(0) = 1/(1 + \tilde{K}_i S_T)^{A_i}$. The independent distributions are thus binomial,

$$\mathbb{P}(a_i) = \frac{A_i!}{(A_i - a_i)!\,a_i!}\left(\frac{\tilde{K}_i S_T}{1 + \tilde{K}_i S_T}\right)^{a_i}\left(\frac{1}{1 + \tilde{K}_i S_T}\right)^{A_i - a_i} \tag{19}$$

with $\mathbb{E}[a_i] = A_i\tilde{K}_i S_T/(1 + \tilde{K}_i S_T)$.

Although we cannot find a concise expression for $\mathbb{E}[a_j/a_s]$, we can approximate it using $\mathbb{E}[a_j]/\mathbb{E}[a_s]$ since it satisfies the same bounds as $\mathbb{E}[a_j/a_s]$ for $a_s \ge 1$. Moreover, in the large S_T limit, we find that $\mathbb{E}[a_1]/\mathbb{E}[a_s] \lesssim \mathbb{E}[a_1/a_s]$ is also a lower bound. Specifically, for the strongest binder A_1,

$$\frac{\mathbb{E}[a_1]}{\mathbb{E}[a_i]} = \frac{A_1}{A_i}\cdot\frac{\tilde{K}_1/(1 + \tilde{K}_1 S_T)}{\tilde{K}_i/(1 + \tilde{K}_i S_T)} \ge \frac{A_1}{A_i}, \tag{20}$$

$$\frac{\mathbb{E}[a_1]}{\mathbb{E}[a_i]} = \frac{A_1\tilde{K}_1}{A_i\tilde{K}_i}\cdot\frac{1/(1 + \tilde{K}_1 S_T)}{1/(1 + \tilde{K}_i S_T)} \le \frac{A_1\tilde{K}_1}{A_i\tilde{K}_i}. \tag{21}$$

Thus, we find

$$\frac{A_1}{A_T} \le \frac{\mathbb{E}[a_1]}{\mathbb{E}[a_s]} \le \frac{A_1\tilde{K}_1}{\sum_{i=1}^M A_i\tilde{K}_i}. \tag{22}$$

When $\tilde{K}_i S_T \gg 1$ for each i, $\mathbb{E}[a_i]$ is approximately A_i, meaning that almost all A_i aptamer molecules are bound. In this limit, the proportion of aptamer A_1 is A_1/A_T, which is invariant before and after SELEX. We will show that it is the theoretical lower bound for the proportion of bound aptamer A_1 if we remove configurations in which no A_1 aptamer is bound.

V. EFFECTIVE TWO-SPECIES MODEL

A. Combining weaker aptamers

In this section, we reduce the multispecies model into an effective two-species model by combining the weaker binding aptamers $A_2, \ldots, A_M$ into one type effective pool A_2'. There are many ways of self-consistently lumping multiple species by constraining specific global quantities. Here, since we focus on the approximation $\mathbb{E}[a_j]/\mathbb{E}[a_s]$ to the expected bound fraction of A_1 proportion after each round of SELEX, we wish the effective two-species model to

preserve the upper and lower bounds of $\mathbb{E}[a_1/a_s|a_s \geq 1]$. If we define the effective association coefficient of the effective pool A_2' by $\bar{K}_2'$, we require

$$\frac{A_1}{A_1 + \sum_{i=2}^{M} A_i} = \frac{A_1}{A_1 + A_2'} \tag{23}$$

and

$$\frac{A_1\bar{K}_1}{A_1\bar{K}_1 + \sum_{i=2}^{M} A_i\bar{K}_i} = \frac{A_1\bar{K}_1}{A_1\bar{K}_1 + A_2'\bar{K}_2'}. \tag{24}$$

Therefore, we find the effective population and association coefficient,

$$A_2' = \sum_{i=2}^{M} A_i, \quad \bar{K}_2' = \frac{\sum_{i=2}^{M} A_i\bar{K}_i}{\sum_{i=2}^{M} A_i}. \tag{25}$$

We henceforth consider this effective two-aptamer model in which the second species can be thought of as an effective species that lumps together all aptamer species except the best binder. Thus, for notational simplicity, we omit the prime symbol, $A_2' \to A_2$ and $\bar{K}_2' \to \bar{K}_2$, and assume $\bar{K}_1 > \bar{K}_2$.

B. Bound aptamer A_1 fraction

We first consider, upon mixing with S_T target molecules, the expected equilibrium fraction of all bound aptamers that are type A_1. The expectation of a_1/a_s is defined only for $a_s = a_1 + a_2 \geq 1$, so we first derive $\mathbb{E}[a_1/a_s \,|\, a_s \geq 1]$. In Sec. IV, we have shown that under the large S_T approximation, $\mathbb{E}[a_1/a_s|a_s \geq 1] = A_1/(A_1 + A_2)$, while under the small S_T approximation, $\mathbb{E}[a_1/a_s \,|\, a_s \geq 1] = A_1\bar{K}_1/(A_1\bar{K}_1 + A_2\bar{K}_2)$. These expected fractions are lower and upper bounds, which we state formally:

Theorem 1. *If $A_1\bar{K}_1/\bar{K}_2$ is an integer, then* $\mathbb{E}[a_1/a_s \,|\, a_s \geq 1] \leq A_1\bar{K}_1/(A_1\bar{K}_1 + A_2\bar{K}_2)$.

Theorem 2. $\mathbb{E}[a_1/a_s \,|\, a_s \geq 1] \geq A_1/(A_1 + A_2)$.

Note that these bounds are equivalent to those obeyed by $\mathbb{E}[a_1]/\mathbb{E}[a_s]$ in the large S_T limit [Eq. (22)]. Here, and in subsequent analyses, we use the specific example values $A_2 = 10A_1$, $\bar{K}_1 = 0.002$, and $\bar{K}_2 = 0.001$. In this setting, we calculate quantities like $\mathbb{E}[a_1/a_s \,|\, a_s \geq 1]$ and plot them in Fig. 2 as functions of S_T and A_1. Even though we have provided analytic approximations for $\mathbb{P}(\mathbf{a})$ under different limits, here, and in subsequent plots of $\mathbb{E}[a_1/a_s]$, we use Eq. (11) to exactly evaluate the expected ratios, except in large-S_T, A_1 regimes where the mass-action approximation is extremely accurate. When A_1 is small and S_T is large, $\mathbb{E}[a_1/a_s \,|\, a_s \geq 1]$ approaches its lower bound $A_1/(A_1 + A_2) = 1/11$. When $S_T = 1$, $\mathbb{E}[a_1/a_s \,|\, a_s \geq 1]$ reaches its upper bound $A_1\bar{K}_1/(A_1\bar{K}_1 + A_2\bar{K}_2) = 1/6$. Notice that $\mathbb{E}[a_1/a_s \,|\, a_s \geq 1]$ is decreasing with S_T but not always increasing with A_1. This deviation from the predictions using the mass-action law reveals the challenge in proving Theorems 1 and 2. We sketch the proofs here and leave the details to Subsection 5 of the Appendix.

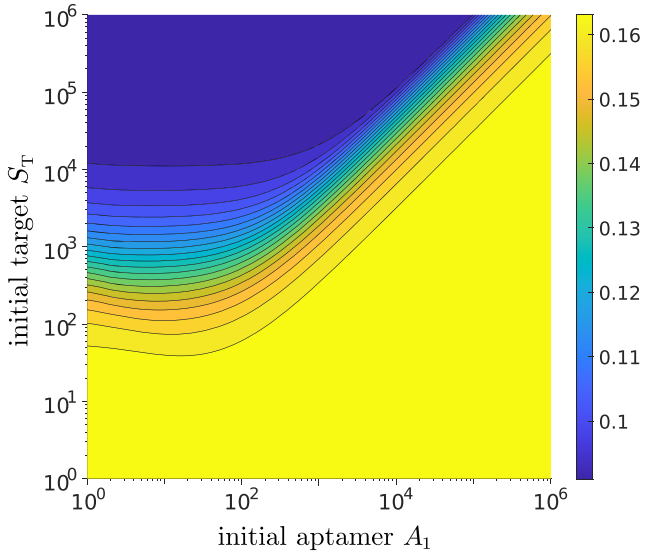

FIG. 2. A density plot of $\mathbb{E}[a_1/a_s \,|\, a_s \geq 1]$ after one round of SELEX that is initiated with S_T and A_1. The initial aptamer A_2 number is $A_2 = 10A_1$ and the association coefficients for A_1, A_2, $\bar{K}_1 = 0.002$, and $\bar{K}_2 = 0.001$, respectively. Here, and in subsequent density plots, we use the mass-action law approximation to compute $\mathbb{E}[a_1/a_s]$ for $A_1 > 200$ and $S_T > 1000$. This leads to faster computation without any discernible difference from the exact result. For even larger $\bar{K}_1/\bar{K}_2$ (relatively weaker A_2 binding), $\mathbb{E}[a_1/a_s \,|\, a_s \geq 1]$ looks qualitatively similar but the contours are shifted upward since fewer targets S_T are needed to capture the same fraction of A_1.

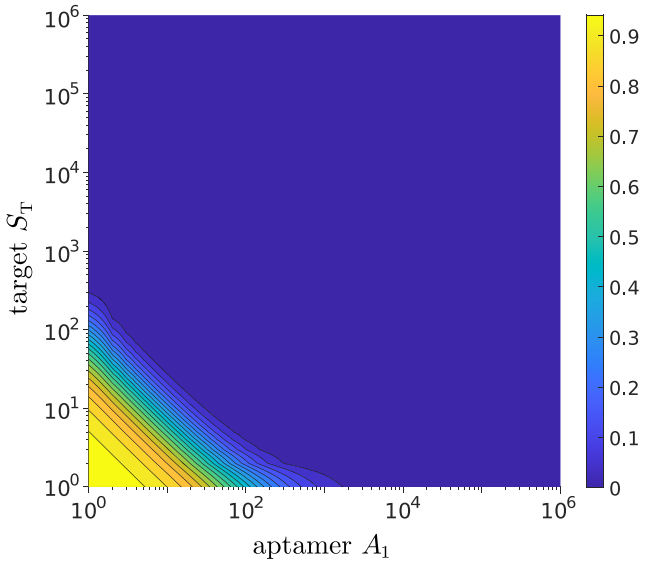

FIG. 3. Density plot of $\mathbb{P}(0,0) \equiv 1/Z$ after one round of SELEX that is initiated with S_T and A_1 targets and A_1 aptamers. The aptamer ratio is set to $A_2 = 10A_1$ and the aptamer-target association coefficients are $\bar{K}_1 = 0.002$ and $\bar{K}_2 = 0.001$. When $A_1 > 200$ and $S_T > 1000$, this probability is smaller than 10^{-10}, and we approximate it as 0. The probability of loss is non-negligible only in the small A_1, S_T corner. As A_T or $\bar{K}_i$ increase, the probability of loss of A_1 (bottom left triangle) decreases and shrinks in extent.

To prove the upper bound $\mathbb{E}[a_1/a_s \,|\, a_s \geq 1] \leq A_1\tilde{K}_1/(A_1\tilde{K}_1 + A_2\tilde{K}_2)$, we consider an alternate system that contains $A_1\tilde{K}_1/\tilde{K}_2$ molecules of aptamer A_1' with association coefficient $\tilde{K}_2$, A_2 molecules of aptamer A_2' with association coefficient $\tilde{K}_2$, and S_T molecules of target. In this system, all aptamers have the same association coefficient. From symmetry, we have $\mathbb{E}[a_1'/a_s' \,|\, a_s' \geq 1] = (A_1\tilde{K}_1/\tilde{K}_2)/(A_1\tilde{K}_1/\tilde{K}_2 + A_2) = A_1\tilde{K}_1/(A_1\tilde{K}_1 + A_2\tilde{K}_2)$, and we prove $\mathbb{E}[a_1/a_s \,|\, a_s \geq 1] \leq \mathbb{E}[a_1'/a_s' \,|\, a_s' \geq 1]$.

For the lower bound $\mathbb{E}[a_1/a_s \,|\, a_s \geq 1] \geq A_1/(A_1 + A_2)$, consider a third system with A_1 molecules of aptamer A_1'' with association coefficient $\tilde{K}_2$, A_2 molecules of aptamer A_2'' with association coefficient $\tilde{K}_2$, and S_T molecules of target. Similarly, $\mathbb{E}[a_1''/a_s'' \,|\, a_s'' \geq 1] = A_1/(A_1 + A_2)$, and we prove $\mathbb{E}[a_1/a_s \,|\, a_s \geq 1] \geq \mathbb{E}[a_1''/a_s'' \,|\, a_s'' \geq 1]$.

We now consider the state with $a_s = 0$. Since we care only about the strongest binder A_1, realizations in which $a_s = a_1 + a_2 = 0$ contribute equivalently to the expectation as the case $a_1 = 0, a_2 \geq 1$. We thus stipulate that the "fraction" $a_1/a_s = 0$ when $a_s = 0$. Thus, we really wish to optimize $\mathbb{E}[a_1/a_s] = \mathbb{E}[a_1/a_s \,|\, a_s \geq 1][1 - \mathbb{P}(0,0)]$, which incorporates the total extinction probability $\mathbb{P}(0,0)$.

Figure 3 shows $\mathbb{P}(0,0) = \mathbb{P}(a_s = 0)$ after one round of SELEX as a function of A_1 (and a corresponding A_2) and S_T. The probability of no bound aptamer decays toward 0 when either A_1 or S_T is large. Now that we have computed $\mathbb{P}(0,0)$, we can evaluate $\mathbb{E}[a_1/a_s]$ and use it to optimize the SELEX strategy.

VI. OPTIMAL SELEX POLICIES

By combining Figs. 2 and 3, we first find $\mathbb{E}[a_1/a_s]$ associated with the first round of SELEX. The upper bound of $\mathbb{E}[a_1/a_s]$ is still $A_1\tilde{K}_1/(A_1\tilde{K}_1 + A_2\tilde{K}_2)$, but since $\mathbb{P}(0,0)$ can be close to 1, the lower bound is very small. Varying the system volume V does not change the bounds of $\mathbb{E}[a_1/a_s]$, since these bounds only depend on A_1/A_2 and $\tilde{K}_1/\tilde{K}_2 = \exp[-\beta(\Delta G_1 - \Delta G_2)]$, both independent of volume. However, smaller V corresponds to larger $\tilde{K}_1$ and $\tilde{K}_2$, and the probability of losing the best binder is smaller.

Figure 4 plots $\mathbb{E}[a_1/a_s]$ after the first round as a function of A_1 (and a corresponding A_2) and S_T. The high-value regions of $\mathbb{E}[a_1/a_s]$ lie in a wide, flat wedge (yellow). The red curve traces the maximum along this plateau and indicates the optimal S_T that maximizes $\mathbb{E}[a_1/a_s]$ for each value of A_1. When S_T is too large, $\mathbb{E}[a_1/a_s]$ approaches $A_1/(A_1 + A_2)$. When A_1 and S_T are too small, the probability of $a_s = 0$ is large, so that $\mathbb{E}[a_1/a_s]$ is small. When A_1 is large, we should take S_T as small as practically allowed to approach the global maximum $A_1\tilde{K}_1/(A_1\tilde{K}_1 + A_2\tilde{K}_2)$. Therefore, for a single round of SELEX, the optimal policy is to use A_1 as large as possible and its associated, small value of S_T.[23]

For the subsequent rounds of SELEX, we can control to some degree the number of targets S_T, the numbers of total aptamer A_1, A_2 (through different levels of amplification), while keeping the ratio A_1/A_2 from the previous round fixed. We now consider feeding in the $A_1/(A_1 + A_2)$ ratio after the first round, described in terms of $\mathbb{E}[a_1/a_s] = \mathbb{E}[a_1/(a_1 + a_2)]$ as input to the second round, and so forth.

Under fixed association coefficients $\tilde{K}_1, \tilde{K}_2$ and an initial ratio A_1/A_2 (used to initiate the first round), a multi-round SELEX policy is defined by a set of values of S_T and A_T (with the relative amounts of aptamers determined by the previous round). In general, we can classify policies into four types:

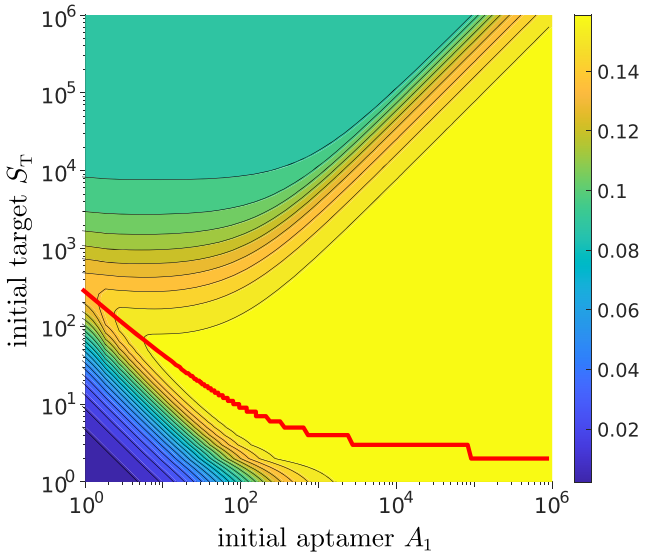

FIG. 4. Density plot of $\mathbb{E}[a_1/a_s]$ after one round of SELEX that is initiated with S_T and A_1. As in Figs. 2 and 3, the ratio is $A_2 = 10A_1$ and the association coefficients are $\tilde{K}_1 = 0.002$ and $\tilde{K}_2 = 0.001$. The red curve traces values of S_T that yield the locally maximal $\mathbb{E}[a_1/a_s]$ for each value of A_1. When A_2 is increased with fixed A_1, the higher aptamer population makes extinction less likely, and $\mathbb{P}(0,0)$ shrinks. Similarly, for larger $\tilde{K}_1/\tilde{K}_2$, fewer targets are required to bind the same fraction of A_1 and achieve the same value of $\mathbb{E}[a_1/a_s]$. Thus, when either A_2 or $\tilde{K}_1/\tilde{K}_2$ is increased, the density plot qualitatively translates downward and the maximum-value curve (red) shifts down to smaller values of S_T.

- Policy 1 results in $\mathbb{E}[a_1/a_s] \approx A_1\tilde{K}_1/(A_1\tilde{K}_1 + A_2\tilde{K}_2)$ and $\mathrm{var}[a_1/a_s] \approx 0$. One example of policy 1 is $A_i \gg S_T^2$ and $S_T \gg 1$.
- Policy 2 yields $\mathbb{E}[a_1/a_s] \approx A_1\tilde{K}_1/(A_1\tilde{K}_1 + A_2\tilde{K}_2)$ and $\mathrm{var}[a_1/a_s] > 0$. One example of policy 2 is $A_i \gg S_T^2$ and $A_i\tilde{K}_i \gg 1$ but $S_T \not\gg 1$.
- Policy 3 gives $\mathbb{E}[a_1/a_s] < A_1\tilde{K}_1/(A_1\tilde{K}_1 + A_2\tilde{K}_2)$ and $\mathrm{var}[a_1/a_s] \approx 0$. One example of policy 3 is $A_T \approx S_T \gg 1$.
- Policy 4 results in $\mathbb{E}[a_1/a_s] < A_1\tilde{K}_1/(A_1\tilde{K}_1 + A_2\tilde{K}_2)$ and $\mathrm{var}[a_1/a_s] > 0$. One example of policy 4 is the large S_T approximation $S_T \gg A_T^2$ without $S_T\tilde{K}_i \gg 1$.

For certain values of $\tilde{K}_1, \tilde{K}_2, A_1/A_2$, policy 1 does not necessarily satisfy $A_i \gg S_T$. For example, if $\tilde{K}_1 = 2 \times 10^{-18}, \tilde{K}_2 = 10^{-18}, A_1/A_2 = 1$, then a policy with $S_T = 10^{15}, A_T = 2 \times 10^6$ is still classified as policy 1. The reason is that only a very small proportion of aptamers is bound, so that for A_1 and A_2, the ratio of their bound probabilities is approximately $\tilde{K}_1/\tilde{K}_2$.

Although policies 1 and 2 are both optimal if performing only one round of SELEX, the optimal policies may change in subsequent rounds. It is important to note that if the ratio A_2/A_1 (or $A_i/\sum_{j=1}^{M} A_j$ in the general case) is determined by a previous round, and policy 1 is then applied, the new expectation $\mathbb{E}[a_1/a_s] = A_1\tilde{K}_1/(A_1\tilde{K}_1 + A_2\tilde{K}_2)$ reaches the upper-bound value, which is independent of total aptamer population A_T. Thus, if policy 1 is applied using a previous-round value of A_2/A_T, the expected fraction will be independent of the amount of PCR amplification after the previous

round and only the resulting fraction A_1/A_T *determined by the previous round* matters.

If we apply policy 1 with $A_i \gg S_T^2$ and $S_T \gg 1$, the law of large numbers implies that $a_1/a_s \approx \mathbb{E}[a_1/a_s] = A_1\tilde{K}_1/(A_1\tilde{K}_1 + A_2\tilde{K}_2)$. Then, after another round of SELEX using policy 1, we use the ratio from round one for the A_1, A_2 in $\mathbb{E}[a_1/a_s] = A_1\tilde{K}_1/(A_1\tilde{K}_1 + A_2\tilde{K}_2)$ to find $A_1\tilde{K}_1^2/(A_1\tilde{K}_1^2 + A_2\tilde{K}_2^2)$ after the second round.

Suppose we had initially applied $A_i \gg S_T^2, A_i\tilde{K}_i \gg 1$ and $S_T = 1$ (policy 2). The first round of SELEX would capture only one aptamer with $\mathbb{E}[a_1/a_s] = A_1\tilde{K}_1/(A_1\tilde{K}_1 + A_2\tilde{K}_2)$ and $\mathrm{var}[a_1/a_s] > 0$. In a subsequent round, since only one aptamer type is left, no further selection is made, and we still have $\mathbb{E}[a_1/a_s] = A_1\tilde{K}_1/(A_1\tilde{K}_1 + A_2\tilde{K}_2)$. The essential difference between policy 1 and policy 2 lies in their different variances of a_1/a_s. Policy 1 is highly deterministic so that $\mathrm{var}[a_1/a_s] \approx 0$, while $\mathrm{var}[a_1/a_s] > 0$ under policy 2. This difference in variance leads to different performances when multiple rounds of SELEX are applied.

In Fig. 5, we plot the expected fraction of bound aptamers that are A_1 after two rounds of SELEX, as a function of the initial values of A_1 and S_T used to initiate the first round. Before round 1 we set $A_2 = 10A_1$, or $A_1/(A_1 + A_2) = 1/11$. After the first round, we apply policy 1. The resulting expectation $\mathbb{E}[a_1/a_s]$ after two rounds is then plotted. We can see that for two rounds of SELEX, applying policy 1 (see the square symbol in Fig. 5 for an example) in round one is much better than applying policies 2, 3, or 4 (e.g., the cross, circle, and triangle symbols in Fig. 5).

After more rounds of SELEX, policy 1 is still better than the other policies. Figure 6 shows $\mathbb{E}[a_1/a_s]$ after three rounds of SELEX

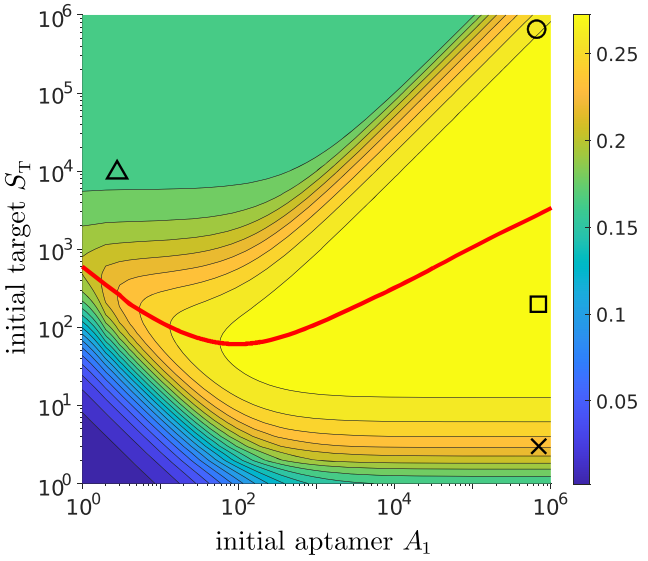

FIG. 5. Density plot of $\mathbb{E}[a_1/a_s]$ after two rounds of SELEX, plotted as a function of S_T and A_1, the target and best-binder numbers that are used to initiate the *first* round. The association coefficients are $\tilde{K}_1 = 0.002$ and $\tilde{K}_2 = 0.001$, and before round one, the ratio of the aptamers is set to $A_2 = 10A_1$. For round 2, we used optimal policy 1. The red curve indicates the location of the maximal proportion for each value of the initial A_1. The square, cross, circle, and triangle symbols denote examples of policies 1–4 applied to round 1, respectively.

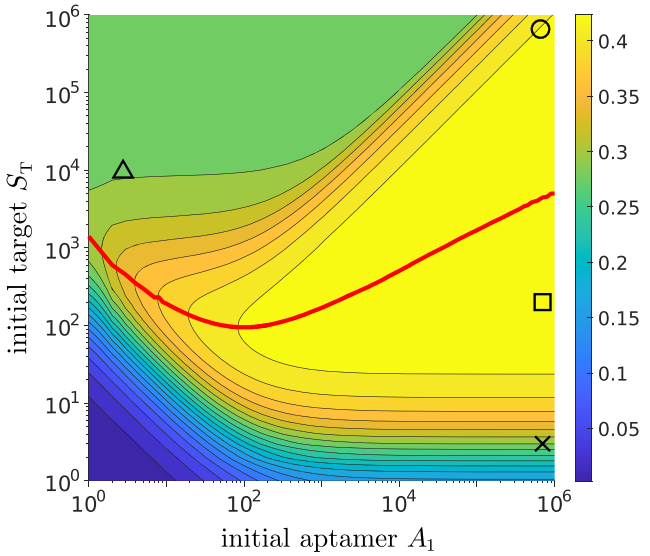

FIG. 6. Density plot of $\mathbb{E}[a_1/a_s]$ after three rounds of SELEX plotted as a function of the initial target and best-binder numbers, S_T and A_1, that are used to initiate the first round. As before, the association coefficients are $\tilde{K}_1 = 0.002$ and $\tilde{K}_2 = 0.001$, and the initial aptamer ratio before round 1 is set to $A_1/(A_1 + A_2) = 1/11$ ($A_2 = 10A_1$). We assumed rounds 2 and 3 both employed optimal policy 1. The red curve indicates the location of the maximal proportion for each value of the initial A_1. The square, cross, circle, and triangle symbols denote examples of policies 1–4 applied to round 1. Note that the high-valued plateau (yellow) stays is a wide wedge (in the initial S_T, A_1 coordinates) and that applying policy 1 throughout (square) yields an expected ratio near its maximum possible value.

as a function of the initial target and aptamer numbers S_T and A_1 used to initiate the first round. We see that the pattern of the expected fraction after three rounds is qualitatively similar to that after two rounds. This arises from performing a recursion on the maximal expected fraction, as detailed in Subsection 6 of the Appendix.

In general, a guideline for the optimal policy is

Theorem 3. *For N rounds of SELEX, to maximize the final expected proportion of aptamer A_1, the optimal policy is to apply policy 1 for the first $N-1$ round and apply either policy 1 or policy 2 for round N.*

We briefly outline the argument and leave the proof to Subsection 6 of the Appendix. For a specific value of binding fraction $r \in [0,1]$, define $f(r) = r\tilde{K}_1/[r\tilde{K}_1 + (1-r)\tilde{K}_2]$. Assume the initial A_1 proportion is r_0. After one and two rounds of policy 1, the A_1 proportion becomes $f(r_0)$ and $f(f(r_0))$, respectively. After one round of policy 2, the A_1 proportion takes on a random value r_1 with $\mathbb{E}[r_1] = f(r_0)$. After two rounds of policy 1, the A_1 proportion becomes $f(f(r_0))$. After two rounds of policy 2, the expected A_1 proportion becomes $f(r_1)$. Since $f(r)$ is concave (downward), by Jensen's inequality, $\mathbb{E}[f(r_1)] \le f(\mathbb{E}[r_1]) = f(f(r_0))$. Therefore, introducing variance to a_1/a_s (e.g., when policy 2 is applied) decreases the final $\mathbb{E}[a_1/a_s]$, and it is better to use additional rounds of SELEX to compensate for this variance effect.

VII. EXTINCTION AND PURIFICATION PROBABILITIES

The "optimal" protocols described above rely on the expectation $\mathbb{E}[a_1/a_s]$ but does not assign a cost associated with losing the best binder, or with not achieving complete purification. During early rounds of SELEX, the highest affinity aptamer may be at very low abundance and there might also be many aptamers that bind nearly as well, outcompeting the best binder. Thus, there is a probability that the best binder A_1 is permanently lost during some cycle. For an effective two-species model, Fig. 7 shows the probability that no A_1 is bound after one round of SELEX, as a function of initial values of A_1 and S_T. When S_T is large enough, $\mathbb{P}(a_1 = 0)$ approaches 0. However, if S_T is small, $\mathbb{P}(a_1 = 0)$ cannot approach 0 for any large A_1, since the number of competing A_2 aptamers also increases.

In the small S_T limit, the extinction probability of A_1 is $\mathbb{P}(a_1 = 0) = (1 - p_1)^{S_T}$, while in the large S_T limit, the extinction probability is $\mathbb{P}(a_1 = 0) = (1 + \bar{K}_1 S_T)^{-A_1}$. Another mixed limit arises when $S_T \ll A_i^2$ for some i. In these cases, we must analyze $\mathbb{P}(a_1 = 0)$ starting from Eq. (7). If we are in the low target regime for the combined number of weak binders $A_2 \gg S_T^2$, but the strongest binder is few in number $A_1 \ll S_T^2$, we can approximate Eq. (11) by

$$\begin{aligned}\mathbb{P}(\mathbf{a}\,|\,\mathbf{A}, S_T) &= \frac{S_T!}{Z(S_T - a_s)!}\prod_{i=1}^{2}\frac{A_i!\,\bar{K}_i^{a_i}}{(A_i - a_i)!\,a_i!}\\ &\approx \frac{S_T!}{Z(S_T - a_s)!}\frac{(A_2\bar{K}_2)^{a_2}}{a_2!}\binom{A_1}{a_1}\bar{K}_1^{a_1}\\ &\approx \binom{S_T - a_1}{a_2}(A_2\bar{K}_2)^{a_2}\frac{S_T^{a_1}}{Z}\binom{A_1}{a_1}\bar{K}_1^{a_1}. \end{aligned} \tag{26}$$

After summing over a_2, we find

$$\sum_{a_2=0}^{S_T - a_1}\mathbb{P}(\mathbf{a}\,|\,\mathbf{A}, S_T) = \frac{(1 + A_2\bar{K}_2)^{S_T - a_1}}{Z}\binom{A_1}{a_1}(S_T\bar{K}_1)^{a_1} \tag{27}$$

and impose $\sum_{a_1=0}^{A_1}\sum_{a_2=0}^{S_T - a_1}\mathbb{P}(\mathbf{a}\,|\,\mathbf{A}, S_T) = 1$ to find

$$Z \approx (1 + A_2\bar{K}_2)^{S_T}\left(1 + \frac{S_T\bar{K}_1}{1 + A_2\bar{K}_2}\right)^{A_1} \tag{28}$$

and

$$\mathbb{P}(a_1\,|\,A_1, A_2, S_T) \approx \frac{\binom{A_1}{a_1}\left(\frac{S_T\bar{K}_1}{1 + A_2\bar{K}_2}\right)^{a_1}}{\left(1 + \frac{S_T\bar{K}_1}{1 + A_2\bar{K}_2}\right)^{A_1}}. \tag{29}$$

The extinction probability is then

$$\mathbb{P}(a_1 = 0\,|\,A_1, A_2, S_T) \approx \left(1 + \frac{S_T\bar{K}_1}{1 + A_2\bar{K}_2}\right)^{-A_1}, \tag{30}$$

which is a good approximation only in the limit $\sqrt{A_2} \gg S_T \gg A_1^2$.

We can also consider the probability of complete purification at some late cycle when all weaker-binding aptamers are lost and only the best binder remains. Figure 8 plots the purification probability $\mathbb{P}(a_1 \geq 1, a_2 = 0)$ as a function of A_1 and S_T of the current cycle. Here, we assume that there remains a small A_2 impurity $A_2 = A_1/50$. To best achieve purification at this later stage, a small S_T and larger

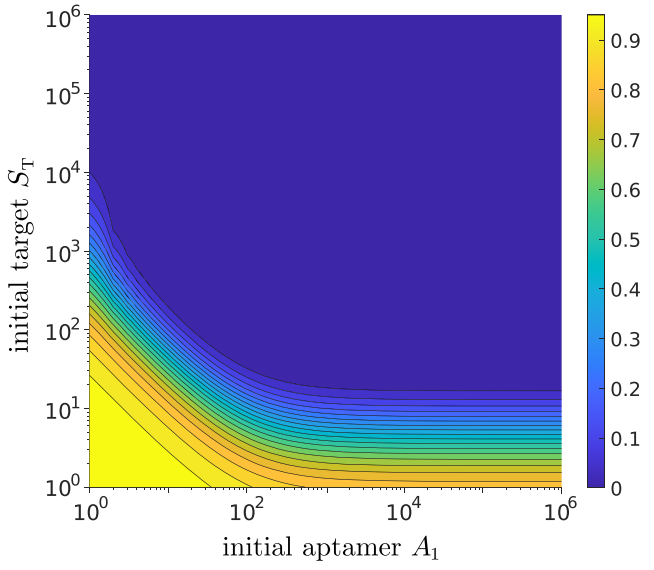

FIG. 7. Density plot of the loss probability $\mathbb{P}(a_1 = 0)$ in a two-species model after one round of SELEX initiated with S_T and A_1. The color measures the probability of no bound aptamer A_1 after one round of SELEX. The initial A_2 aptamer abundance is set to $A_2 = 10A_1$ and the association coefficients are $\bar{K}_1 = 0.002$ and $\bar{K}_2 = 0.001$. When $A_1 > 200$ and $S_T > 1000$, the loss probability is smaller than 10^{-10}, and we neglect it.

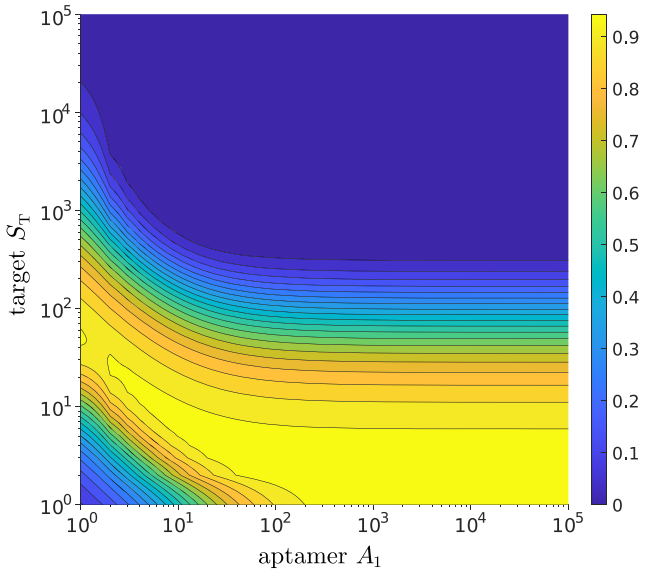

FIG. 8. Density plot of the purification probability $\mathbb{P}(a_1 \geq 1, a_2 = 0)$ as a function of S_T and $A_1 = 50A_2$. Here, $\bar{K}_1 = 0.002 = 2\bar{K}_2$ and we are considering a later round of SELEX in which the aptamer A_1 has been well isolated, but with ~2% A_2 impurity. When $A_2 > 100$ and $S_T > 1000$, $\mathbb{P}(a_1 \geq 1, a_2 = 0) < 10^{-4}$, which we approximate as zero.

aptamer population (even there may be larger total numbers of A_2) is indicated. In the limit $\sqrt{A_1} \gg S_T \gg A_2^2$, we can use the relevant approximations to find

$$\mathbb{P}(a_1 \geq 1, a_2 = 0) \approx \frac{(1 + A_1\tilde{K}_1)^{S_T} - 1}{(1 + A_1\tilde{K}_1)^{S_T}\left(1 + \frac{S_T\tilde{K}_2}{1+A_1\tilde{K}_1}\right)^{A_2}}. \quad (31)$$

These loss and purification probabilities add extra dimensions to SELEX optimization strategy. For example, in addition to round-wise maximization of the expected fraction of best-binder $\mathbb{E}[a_1/a_s]$, there might be a great cost associated with loss of the best binder, or great utility gained with complete purification. Thus, one can imagine that besides $\mathbb{E}[a_1/a_s]$, we can develop round-dependent objective functions that include some combination of $\mathbb{E}[a_1/a_s]$, $\mathbb{P}(a_1 = 0)$, and/or $\mathbb{P}(a_1 \geq 1, a_2 = 0)$. Depending on their weighting, the overall optimal policy may result in a sequence of S_T that changes over different rounds. If we include a penalty for the loss (Fig. 7), to avoid extinction of A_1, the optimal policy will be shifted slightly upward in S_T, while to reward purification (Fig. 8), the optimal S_T will be lowered during later rounds. However, since comparably large values of $\mathbb{E}[a_1/a_s]$ arise over a wide wedge of S_T, A_1 values, these considerations are not expected to dramatically change the optimization policy unless very large loss penalties or high purification rewards are demanded.

VIII. DISCUSSION AND CONCLUSIONS

The statistical mechanical model that we derived in Sec. II yields the equilibrium configurations that, in the large system limit, are consistent with the solutions of the mass action model proposed by Wang *et al.*[11] More importantly, it allows the study of low target or aptamer concentration scenarios where stochastic effects cannot be ignored. We then used our results to investigate the optimal policy for maximizing the fraction of the best binder. For one round of SELEX, the mass action model and the stochastic model both indicate that S_T should be as small as feasibly possible, and we proved that in this low-target limit, $\mathbb{E}[a_1/a_s]$ reaches its upper bound $A_1\tilde{K}_1/(A_1\tilde{K}_1 + A_2\tilde{K}_2)$. Nevertheless, we argued that the optimal policy is $A_i \gg S_T^2$ and $S_T \gg 1$, if we want more than one round of SELEX. In Subsection 1 of the Appendix, we discuss a scenario in which the binding is irreversible and prove related bounds for the expected proportion of the best binder.

In our analysis, some quantities were not thoroughly studied, such as the probability that the proportion of the best binder exceeds a threshold or the probability that the weighted ΔG_i exceeds a threshold. These quantities might not have explicit expressions, and calculating them numerically might also be challenging. Note that our results are based on simple second-order binding and spontaneous dissociation, parameterized by the association coefficient $\tilde{K}_i$. We also propose that more complex binding schemes that involve intermediate steps that dissipate free energy and participate in kinetic proofreading can be molecularly designed.[24] If such intermediate-stage kinetics can be integrated into the target-aptamer binding process, a level of control on $\tilde{K}_i$ can be imparted, including amplification of the contrast in $\tilde{K}_i$ or an effective reconfiguration of the association coefficients. However, note that SELEX concerns a population evolution process at equilibrium, while the kinetic proofreading considers a non-equilibrium process for each target-aptamer pair affecting the parameters $\tilde{K}_i$ within SELEX.

While we focused on stationary behavior, more general time-dependent results can be developed via a continuous-time Markov process, which might be represented by, e.g., a high-dimensional master equation. The Markov process describing the mixing of aptamers and targets would then be stopped at a finite time before their binding dynamics reach equilibrium. When considering the full kinetics, not just its stationary distribution, tools such as Kurtz's theorem[25] and random time-change representation[26] may prove useful. The high-dimensional master equation can also be analyzed using simulations or semi-analytic approaches such as large system size expansions[27] or large deviation/WKB methods.[28] Quantities that vanish at equilibrium, such as entropy production,[18] can also be studied. Along these lines, we consider a scenario in which the strongest binder A_1 has much faster binding and unbinding rates than other aptamers. Then, we expect a time window in which the binding of A_1 is close to equilibrium, while other aptamer types remain mostly unbound. Stopping the reaction within this time window can greatly increase the proportion of bound A_1, to a degree exceeding even the theoretical upper bound in Theorem 1. The corresponding "irreversible" binding scenario presented in Subsection 1 of the Appendix also can be regarded as stopping the process before reaching equilibrium.

Based on mass action models, many variants of SELEX have been studied.[12,14–17] Stochastic approaches can be extended to these more complex selection scenarios[29] but are much more difficult to analyze. For example, some protocols call for the addition of another type of target substrate that binds non-specifically to aptamers.[14,17] In this aptamer-target-substrate system, the optimal policy is much more complicated. Other SELEX scenarios include multiple, simultaneous target types.[12,15] Since different target molecules prefer different aptamers, multiple aptamers may be selected after multiple rounds of SELEX. Our mathematical analysis assumed positive SELEX, where bound aptamers are kept for amplification. If one wishes to isolate and purify the weakest binding aptamer, we can apply "negative SELEX," where the unbound aptamers are kept for amplification, and the bound aptamers are abandoned. If we consider two target types, S_1 and S_2, and the goal is to select an aptamer that binds strongly to S_1 but that not binds to S_2, we can apply "alternating SELEX," where positive SELEX is performed using S_1, followed by negative SELEX using S_2. Alternating the positive and negative SELEX over multiple rounds, one can expect to isolate the molecule that strongly interacts with one target but is inert to another. Here, determining the optimal SELEX protocol is more complicated,[16] particularly in the stochastic limit.

Although we formulated our model and results in the context of molecular SELEX, our results can be straightforwardly adapted to other evolution problems that involve sequential episodes of selection. Applications with steps that are analogous to isolating a strongest binder are cell sorting,[30] immune selection,[31] or the selection of drug-resistant or cancer cells from a heterogeneous population.[32,33] For example, an initial heterogeneous population of cells may carry different resistances to a certain drug. If the goal is to separate the phenotype with the highest drug resistance, one can apply a process that is similar to SELEX: add a certain level of drug, harvest surviving cells, and then cultivate these surviving cells

to amplify their population size. Higher drug levels correspond to a smaller target number of S_T in SELEX, meaning that fewer cells survive, and the expected proportion of the most resistant cell type is higher after each round. However, when the drug level is too high, it is possible that the most resistant type does not survive. When the drug level is too low, almost no cells are killed, corresponding to the large S_T approximation in SELEX. In general, the optimal policy is to set the drug level relatively high, but not too high to extinguish the most resistant cell type. Finally, the generation of new aptamers from the intrinsic stochastic error of the PCR process also renders the SELEX protocol a molecular evolution problem. These applications and their rich mathematical extensions will be the subject of future investigation.

ACKNOWLEDGMENTS

This work was supported by grants from the NIH through Grant No. R01HL146552 and the NSF through Grant No. DMS-1814364.

AUTHOR DECLARATIONS

Conflict of Interest

The authors have no conflicts to disclose.

Author Contributions

Yue Wang: Conceptualization (supporting); Formal analysis (lead); Investigation (equal); Methodology (equal); Software (equal); Visualization (equal); Writing – original draft (equal); Writing – review and editing (equal). **Bhaven A. Mistry:** Conceptualization (supporting); Formal analysis (lead); Investigation (supporting); Methodology (equal); Writing – original draft (equal). **Tom Chou:** Conceptualization (equal); Formal analysis (supporting); Funding acquisition (lead); Investigation (equal); Methodology (supporting); Project administration (lead); Supervision (lead); Writing – original draft (equal); Writing – review and editing (equal).

DATA AVAILABILITY

Data sharing is not applicable to this article as no new data were created or analyzed in this study.

APPENDIX: MATHEMATICAL APPENDICES

1. Irreversible binding regime

Consider the irreversible binding limit when aptamers, once bound to a target molecule, do not dissociate. The reaction scheme is, thus, described by

$$\mathrm{A}_i + \mathrm{S} \rightharpoonup \mathrm{A}_i\mathrm{S}.$$

Here, we cannot use a detailed balance and then let detachment rates $\to 0^+$ as this is a singular limit that leads to qualitatively different results from the strict no-detachment case.[34,35] However, we can still employ Markov chains or solve the high-dimensional master equations to find probability distributions at finite times.

We study the distribution of bound aptamers after all possible irreversible reactions have been fully realized and there are no longer both free aptamers and free targets. This singular binding-only limit might not be strictly realistic in the context of aptamer binding and selection where molecular unbinding, if even extremely slow, is inevitable. Nonetheless, we expect an intermediate timescale to arise during which nearly all binding reactions have occurred yet no unbinding has happened. Therefore, within this timescale, a strictly irreversible kinetics model is useful but cannot be analyzed using equilibrium statistical mechanics. Notice that the distribution of bound aptamers depends on the activation energy G_i^+ of binding but not the activation energy of unbinding $G_i^- \to \infty$.

We start by defining a kinetic attempt frequency ω_i and the aptamer-target binding rate $r_i = \omega_i \exp(-\beta G_i^+)$. We order the aptamers such that $r_1 \geq r_2 \geq \ldots \geq r_M$, defining A_1 as the fastest binder. The probability that one target molecule binds to aptamer A_i will, thus, be proportional to r_i. Since the binding is irreversible, we can treat target molecules one by one. If the current numbers of unbound aptamers are $\tilde{a}_1, \ldots, \tilde{a}_M$ and $\sum_{j=1}^M \tilde{a}_j > 0$, then the probability that the just-added target binds to aptamer A_i is $\tilde{a}_i r_i / (\sum_{j=1}^M \tilde{a}_j r_j)$. If this target binds to aptamer A_i, then the probability that the next target binds to aptamer A_j is $\tilde{a}_j r_j / [\tilde{a}_1 r_1 + \cdots + (\tilde{a}_i - 1) r_i + \cdots + \tilde{a}_M r_M]$.

Now assume that we start with a single target $S_T = 1$ and that the total initial number of aptamers is $\mathbf{A} = (A_i, \ldots, A_M)$. The probability that the target binds to aptamer A_1 is, thus, $A_1 r_1 / (\sum_{j=1}^M A_j r_j)$. In the high target limit $S_T \geq \sum_{j=1}^M A_j$, all aptamers will eventually be bound and the expected fraction of targets that are bound to A_1 is simply $A_1 / (\sum_{j=1}^M A_j)$. We shall prove that for any number of targets S_T, these values are the upper and lower bounds for the expected fraction of A_1-bound targets.

Theorem 4. *When binding is irreversible, for a given* $\mathbf{A}$ *and different* S_T, *the expected fraction of target that is bound to* A_1 *falls between* $A_1 / (\sum_{j=1}^M A_j)$ *and* $A_1 r_1 / (\sum_{j=1}^M A_j r_j)$.

Proof. We add one target molecule into the pool of aptamers. After this target has bound to an aptamer, we successively add target molecules, one at a time. Given $\mathbf{A} = (A_1, \ldots, A_M)$, denote the probability that the ith target molecule added binds to aptamer A_1 by $\mathbb{P}(i)$. We can assume that the total target number S_T satisfies $S_T \leq \sum_{j=1}^M A_j$ and construct the expected fraction of targets bound to aptamer A_1 as $\mathbb{E}[a_1/S_T \,|\, S_T] = S_T^{-1} \sum_{i=1}^{S_T} \mathbb{P}(i)$. If we can prove that $\mathbb{P}(i)$ is non-increasing, then $\mathbb{E}[a_1/S_T \,|\, S_T]$ is also non-increasing in S_T. Since $\mathbb{E}[a_1/S_T \,|\, S_T = 1] = A_1 r_1 / (\sum_{j=1}^M A_j r_j)$ and $\mathbb{E}[a_1/S_T \,|\, S_T = \sum_{j=1}^M A_j] = A_1 / (\sum_{j=1}^M A_j)$, these values become the desired bounds. Thus, we need only to prove $\mathbb{P}(k) \geq \mathbb{P}(k+1)$.

Assume that before adding the kth target $(k \geq 1)$, the numbers of unbound aptamers are $\tilde{\mathbf{a}} \equiv (\tilde{a}_1, \ldots, \tilde{a}_M)$. If $\tilde{a}_1 = 0$, then $\mathbb{P}(k \,|\, \mathbf{a}) = \mathbb{P}(k+1 \,|\, \mathbf{a}) = 0$. For all other $\tilde{\mathbf{a}}$, we find

$$\begin{aligned} \mathbb{P}(k|\tilde{\mathbf{a}}) &= \frac{\tilde{a}_1 r_1}{\sum_{j=1}^M \tilde{a}_j r_j}, \\ \mathbb{P}(k+1|\tilde{\mathbf{a}}) &= \frac{\tilde{a}_1 r_1}{\sum_{j=1}^M \tilde{a}_j r_j} \cdot \frac{(\tilde{a}_1 - 1) r_1}{\left(\sum_{j=1}^M \tilde{a}_j r_j\right) - r_1} \\ &\quad + \sum_{i=2}^M \frac{\tilde{a}_i r_i}{\sum_{j=1}^M \tilde{a}_j r_j} \cdot \frac{\tilde{a}_1 r_1}{\left(\sum_{j=1}^M \tilde{a}_j r_j\right) - r_i}. \end{aligned} \tag{A1}$$

Here, the summation skips index i if $\tilde{a}_i = 0$. Upon taking the difference and defining $R(\tilde{\mathbf{a}}) \equiv \sum_{j=1}^{M} \tilde{a}_j r_j$, we find

$$\begin{aligned}
&\mathbb{P}(k\,|\,\tilde{\mathbf{a}}) - \mathbb{P}(k+1\,|\,\tilde{\mathbf{a}}) \\
&\quad = \frac{\tilde{a}_1 r_1}{R(\tilde{\mathbf{a}})}\left[1 - \frac{(\tilde{a}_1 - 1)r_1}{R(\tilde{\mathbf{a}}) - r_1} - \sum_{i=2}^{M} \frac{\tilde{a}_i r_i}{R(\tilde{\mathbf{a}}) - r_i}\right] \\
&\quad = \frac{\tilde{a}_1 r_1}{R(\tilde{\mathbf{a}})}\left[\frac{R(\tilde{\mathbf{a}})}{R(\tilde{\mathbf{a}}) - r_1} - \frac{\tilde{a}_1 r_1}{R(\tilde{\mathbf{a}}) - r_1} - \sum_{i=2}^{M} \frac{\tilde{a}_i r_i}{R(\tilde{\mathbf{a}}) - r_i}\right] \\
&\quad = \frac{\tilde{a}_1 r_1}{R(\tilde{\mathbf{a}})}\left[\sum_{i=1}^{M} \frac{\tilde{a}_i r_i}{R(\tilde{\mathbf{a}}) - r_1} - \sum_{i=1}^{M} \frac{\tilde{a}_i r_i}{R(\tilde{\mathbf{a}}) - r_i}\right] \\
&\quad = \frac{\tilde{a}_1 r_1}{R(\tilde{\mathbf{a}})} \sum_{i=1}^{M} \frac{\tilde{a}_i r_i}{R(\tilde{\mathbf{a}}) - r_1}\left(\frac{r_1 - r_i}{R(\tilde{\mathbf{a}}) - r_i}\right) \geq 0. \qquad \text{(A2)}
\end{aligned}$$

Here, the summation skips index i if $\tilde{a}_i = 0$. This last relation stems from the definition that $r_1 \geq r_i$ and $R(\tilde{\mathbf{a}}) > r_i$, rendering the last term always non-negative. Thus, we have shown that for all feasible $\tilde{\mathbf{a}}$ just before the addition of the kth and $(k+1)$th targets, $\mathbb{P}(k\,|\,\tilde{\mathbf{a}}) \geq \mathbb{P}(k+1\,|\,\mathbf{a})$, and hence, $\mathbb{P}(k)$ is non-increasing in k. The expected fraction of targets bound to A_1 aptamer, thus, decreases monotonically from its maximum value $\mathbb{E}[a_1/S_T\,|\,S_T = 1] = A_1 r_1/(\sum_{j=1}^{M} A_j r_j)$ to its minimum value $\mathbb{E}[a_1/S_T\,|\,S_T = \sum_{j=1}^{M} A_j] = A_1/(\sum_{j=1}^{M} A_j)$. As is with the equilibrium problem described in the main text, the expected bound A_1 fraction under irreversible kinetics exhibits similar upper and lower bounds. Since the irreversible scenario is relatively easy to analyze, this proof is relatively straightforward.

□

2. Proof of Eq. (5)

Assume that there are A_i molecules of aptamer A_i. First, freeze the configurations of the aptamers $A_2, \ldots, A_M$ and study the dynamics of aptamer A_1. Define s' as the number of targets that are either free or bound to A_1 aptamers. For the Markov chain of aptamer A_1, the state space $\{(x,y,z)\}$ describes x A_1 aptamer molecules that are not within the dimerization volume of those s' targets, y A_1 aptamers that are within the dimerization volume of those s' targets but not bound, and z aptamers that are bound. Since A_1 aptamers can only be in one of these three states, $x + y + z = A_1$.

The ratio of the transition rates connecting states (x,y,z) and $(x,y-1,z+1)$ is

$$\frac{r[(x,y,z) \to (x,y-1,z+1)]}{r[(x,y-1,z+1) \to (x,y,z)]} = \frac{y(s'-z)/s'}{z+1} e^{-\beta \Delta G_1}, \qquad \text{(A3)}$$

where ΔG_1 is the activation energy of binding and $y(s'-z)/s'$ is the expected number of A_1 aptamer molecules, which are within the dimerization volume of targets that are not bound (z of s' targets are bound to aptamer A_1). The ratio of transition rates between (x,y,z) and $(x-1,y+1,z)$ is

$$\frac{r[(x,y,z) \to (x-1,y+1,z)]}{r[(x-1,y+1,z) \to (x,y,z)]} = \frac{x s' v}{(y+1)(V - s'v)}. \qquad \text{(A4)}$$

The transitions in Eq. (A4) arise from diffusion and are proportional to the available phase space volumes.

We can verify that this Markov chain satisfies detailed balance, so that the ratio of transition rates is the ratio of stationary probabilities. Using the constraint $x + y = A_1 - z$, we can use Eq. (A4) to find

$$\mathbb{P}(i, A_1 - z - i, z) = \mathbb{P}(0, A_1 - z, z)\binom{A_1 - z}{i}\left(\frac{V - s'v}{s'v}\right)^i \qquad \text{(A5)}$$

so that

$$\mathbb{P}(z) := \sum_{i=0}^{A_1 - z} \mathbb{P}(i, A_1 - z - i, z) = \mathbb{P}(0, A_1 - z, z)\left(\frac{V}{s'v}\right)^{A_1 - z}. \qquad \text{(A6)}$$

From Eq. (A3), we find

$$\mathbb{P}(0, A_1 - z - 1, z + 1) = \mathbb{P}(0, A_1 - z, z)\frac{(s'-z)(A_1 - z)}{s'(z+1)} e^{-\beta \Delta G_1}, \qquad \text{(A7)}$$

which leads to

$$\begin{aligned}
\mathbb{P}(i, A_1 - z - 1 - i, z + 1) &= \mathbb{P}(0, A_1 - z, z)\frac{(s'-z)(A_1 - z)}{s'(z+1)} \\
&\quad \times e^{-\beta \Delta G_1}\binom{A_1 - z - 1}{i}\left(\frac{V - s'v}{s'v}\right)^i. \qquad \text{(A8)}
\end{aligned}$$

Thus, we find

$$\begin{aligned}
\mathbb{P}(z+1) &:= \sum_{i=0}^{A_1 - z - 1} \mathbb{P}(i, A_1 - z - 1 - i, z + 1) \\
&= \mathbb{P}(0, A_1 - z, z)\frac{(s'-z)(A_1 - z)}{s'(z+1)} \\
&\quad \times e^{-\beta \Delta G_1}\left(\frac{V}{s'v}\right)^{A_1 - z - 1} \qquad \text{(A9)}
\end{aligned}$$

and, finally,

$$\frac{\mathbb{P}(z+1)}{\mathbb{P}(z)} = \frac{(s'-z)(A_1 - z)}{z+1}\frac{v}{V} e^{-\beta \Delta G_1}. \qquad \text{(A10)}$$

In this new Markov chain, the transition rates can be clearly interpreted. With z bound A_1 aptamers, there are $s' - z$ unbound targets and $A_1 - z$ unbound aptamers that can bind. Each of the $z + 1$ bound A_1 aptamers can dissociate. These two processes are balanced by the association coefficient $\tilde{K}_1 = (v/V)\exp(-\beta \Delta G_1)$.

We can also combine states for the other aptamers. Assume that there are a_i bound A_i aptamers and define $a_s = \sum_{i=1}^{M} a_i$. The ratio of transition rates between $(a_1, \ldots, a_i, \ldots, a_M)$ and $(a_1, \ldots, a_i + 1, \ldots, a_M)$ is then

$$\frac{r[\mathbf{a} \to (a_1, \ldots, a_i + 1, \ldots, a_M)]}{r[(a_1, \ldots, a_i + 1, \ldots, a_M) \to \mathbf{a}]} = \frac{(S_T - a_s)(A_i - a_i)}{a_i + 1}\tilde{K}_i, \qquad \text{(A11)}$$

where $\tilde{K}_i := (v/V)\exp(-\beta \Delta G_i)$. We can verify that this Markov chain on $(\mathbb{Z}^*)^M$ satisfies detailed balance, so that the stationary probability becomes that given in Eq. (7).

3. Proof that $[a_1]/[a_s]$ decreases with $[S_T]$ and increases with $[A_T]$

Lemma 1. Fix $[A_i]$ *and increase the concentration of targets from* $[S_T]$ *to* $[S_T]'$. *After reaching the new equilibrium, the new value* $[\bar{s}]' > [\bar{s}]$.

Proof. Assume that at the new equilibrium, $[a_i]$ becomes $[a_i]'$, and $[\bar{s}]$ becomes $[\bar{s}]'$. Recall Eq. (10),

$$[a_i] = \frac{[A_i]K_i}{K_i + 1/[\bar{s}]}. \tag{A12}$$

If $[\bar{s}]' \le [\bar{s}]$, then $[a_i]' \le [a_i]$ for each i, meaning that $[S_T]' = [\bar{s}]' + \sum_{i=1}^{M}[a_i]' \le [\bar{s}] + \sum_{i=1}^{M}[a_i] = [S_T]$, thus contradicting the assumption $[S_T]' > [S_T]$. □

Lemma 2. Fix $[S_T]$ *and increase the number of aptamers from* $[A_T]$ *to* $[A_T]'$ *while keeping the relative proportions of* $[A_i]$ *fixed, i.e., every* $[A_i]$ *is multiplied by a common factor:* $[A_i]' = ([A_T]'/[A_T]) \times [A_i]$. *At the new equilibrium, the new value* $[\bar{s}]' < [\bar{s}]$.

Proof. If $[\bar{s}]' \ge [\bar{s}]$, then $[a_i]' > [a_i]$ and $[\bar{s}]' = [S_T] - \sum_{i=1}^{M}[a_i]' < [S_T] - \sum_{i=1}^{M}[a_i] = [\bar{s}]$, presenting a contradiction. □

Now, consider how $[a_1]/[a_s]$ changes upon decreasing $[S_T]$ and/or increasing $[A_T]$. Since all $[A_i]$ are multiplied by the same factor when $[A_T]$ is increased, this factor cancels in the fraction

$$\frac{[a_1]'}{[a_s]'} = \frac{\frac{[A_1]'K_1}{K_1+1/[\bar{s}]'}}{\sum_{i=1}^{M}\frac{[A_i]'K_i}{K_i+1/[\bar{s}]'}} = \frac{\frac{[A_1]K_1}{K_1+1/[\bar{s}]'}}{\sum_{i=1}^{M}\frac{[A_i]K_i}{K_i+1/[\bar{s}]'}} \tag{A13}$$

so that the only change in the expression for $[a_1]/[a_s]$ is $[\bar{s}] \to [\bar{s}]'$. The expression for $[a_1]/[a_s]$ can also be rewritten in the following form:

$$\begin{aligned}\frac{[a_1]}{[a_s]} &= \frac{\frac{[A_1]K_1}{K_1+1/[\bar{s}]}}{\sum_{i=1}^{M}\frac{[A_i]K_i}{K_i+1/[\bar{s}]}} \\ &= \frac{\frac{[A_1]K_1}{K_1+1/[\bar{s}]'}\left(\frac{K_1+1/[\bar{s}]'}{K_1+1/[\bar{s}]}\right)}{\sum_{i=1}^{M}\frac{[A_i]K_i}{K_i+1/[\bar{s}]'}\left(\frac{K_i+1/[\bar{s}]'}{K_i+1/[\bar{s}]}\right)} \\ &\equiv \frac{\frac{[A_1]K_1}{K_1+1/[\bar{s}]'}}{\sum_{i=1}^{M}\frac{[A_i]K_i}{K_i+1/[\bar{s}]'}\,\gamma_i},\end{aligned} \tag{A14}$$

where

$$\gamma_i \equiv \left(\frac{K_i + 1/[\bar{s}]'}{K_i + 1/[\bar{s}]}\right)\left(\frac{K_1 + 1/[\bar{s}]}{K_1 + 1/[\bar{s}]'}\right). \tag{A15}$$

From the last equality in Eq. (A14), we see that $[a_1]/[a_s]$ is precisely $[a_1]'/[a_s]'$ if $\gamma_i = 1$. However, since we ordered the aptamers by decreasing affinity, $K_1 \ge K_{i\ge 2}$, and $[\bar{s}]' < [\bar{s}]$, we have $\gamma_i < 1$. Thus, the RHS of Eq. (A14), and hence $[a_1]/[a_s]$, is greater than $[a_1]'/[a_s]'$.

4. Details of the small S_T approximation

In the small S_T limit, since

$$\begin{aligned}a_1\mathbb{P}(\mathbf{a}) = &\frac{p_1 S_T (S_T-1)!}{(S_T-a_s)!\,(a_1-1)!\prod_{i=2}^{M}a_i!} \\ &\times p_0^{S_T-a_s}p_1^{a_1-1}\prod_{i=2}^{M}p_i^{a_i},\end{aligned} \tag{A16}$$

we find $\mathbb{E}[a_i] = p_i S_T$, and since

$$\begin{aligned}a_1(a_1-1)\mathbb{P}(\mathbf{a}) = &\frac{p_1^2 S_T (S_T-1)(S_T-2)!}{(S_T-a_s)!\,(a_1-2)!\prod_{i=2}^{M}a_i!} \\ &\times p_0^{S_T-a_s}p_1^{a_1-2}\prod_{i=2}^{M}p_i^{a_i},\end{aligned} \tag{A17}$$

we find $\mathbb{E}[a_i(a_i-1)] = p_i^2 S_T(S_T-1)$. Thus, $\mathbb{E}[a_i^2] = p_i^2 S_T^2 + p_i(1-p_i)S_T$ and $\mathrm{var}(a_i) = p_i(1-p_i)S_T$. For the correlation coefficient, since

$$\begin{aligned}a_1a_2\mathbb{P}(\mathbf{a}) = &\frac{p_1p_2 S_T (S_T-1)(S_T-2)!}{(S_T-a_s)!\,(a_1-1)!\,(a_2-1)!\prod_{i=3}^{M}a_i!} \\ &\times p_0^{S_T-a_s}p_1^{a_1-1}p_2^{a_2-1}\prod_{i=3}^{M}p_i^{a_i},\end{aligned} \tag{A18}$$

we find, in general, $\mathbb{E}[a_ia_j] = p_ip_jS_T(S_T-1)$ and

$$\mathrm{corr}(a_i,a_j) = -\sqrt{\frac{p_ip_j}{(1-p_i)(1-p_j)}}. \tag{A19}$$

Specifically, for two aptamer species and $p_0 \ll 1$, nearly every target is bound to either aptamer A_1 or aptamer A_2, so that $p_1 + p_2 \approx 1$, $a_1 + a_2 \approx S_T$, and $\mathrm{corr}(a_1,a_2) \approx -1$. Two random variables with a fixed sum have correlation coefficient -1.

5. Proofs of Theorem 1 and Theorem 2

To prove the upper bound $\mathbb{E}[a_1/a_s \,|\, a_s \ge 1] \le A_1\tilde{K}_1/(A_1\tilde{K}_1 + A_2\tilde{K}_2)$, we compare with another system containing $A_1\tilde{K}_1/\tilde{K}_2$ molecules of aptamer A_1' with association coefficient $\tilde{K}_2$, A_2 molecules of aptamer A_2' with association coefficient $\tilde{K}_2$, and S_T molecules of the target. In this comparison system, all aptamers have the same association coefficient. Due to symmetry, in the new system, we apparently have $\mathbb{E}[a_1'/a_s' \,|\, a_s' \ge 1] = (A_1\tilde{K}_1/\tilde{K}_2)/(A_1\tilde{K}_1/\tilde{K}_2 + A_2) = A_1\tilde{K}_1/(A_1\tilde{K}_1 + A_2\tilde{K}_2)$. What remains is to prove that $\mathbb{E}[a_1/a_s \,|\, a_s \ge 1] \le \mathbb{E}[a_1'/a_s' \,|\, a_s' \ge 1]$. To do so requires the following three-part lemma:

Lemma 3. (1) *Consider the sequences*

$$q_0, q_1, \ldots, q_n > 0 \quad \text{and} \quad q_0', q_1', \ldots, q_n' > 0$$

with $\sum_{i=0}^{n} q_i = \sum_{i=0}^{n} q_i' = 1$. *For* $i = 0, 1, \ldots, n-1$, *assume*

$$q_i' q_{i+1} \le q_{i+1}' q_i.$$

In addition, consider the sequences

$$c_0 \le c_1 \le \ldots \le c_n \quad \text{and} \quad c_0' \le c_1' \le \ldots \le c_n'$$

with $c_i \le c_i'$ for $i = 0, 1, \ldots, n$. Then,

$$\sum_{i=0}^{n} q_i c_i \le \sum_{i=0}^{n} q_i' c_i'.$$

(2) If $c_i \ge c_i'$, $c_0 \le c_1 \le \ldots \le c_n$, $c_0' \le c_1' \le \ldots \le c_n'$, and $q_i' q_{i+1} \ge q_{i+1}' q_i$, then $\sum_{i=0}^{n} q_i c_i \ge \sum_{i=0}^{n} q_i' c_i'$.
(3) If $c_i \le c_i'$, $c_0 \ge c_1 \ge \ldots \ge c_n$, $c_0' \ge c_1' \ge \ldots \ge c_n'$, and $q_i' q_{i+1} \ge q_{i+1}' q_i$, then $\sum_{i=0}^{n} q_i c_i \le \sum_{i=0}^{n} q_i' c_i'$.

Proof. Since $q_i' q_{i+1} \le q_{i+1}' q_i$, if $q_i' \ge q_i$, then $q_{i+1}' \ge q_{i+1}$. Thus, there is an index k such that $q_i' \le q_i$ for $i = 0, 1, \ldots, k$ and $q_i \ge q_i$ for $i = k+1, \ldots, n$. Set $u_i = q_i' - q_i$, then $\sum_{i=0}^{n} u_i = 0$. We have $u_i \le 0$ for $i = 0, 1, \ldots, k$ and $u_i \ge 0$ for $i = k+1, \ldots, n$. Then,

$$\begin{aligned}\sum_{i=0}^{n} q_i' c_i' - \sum_{i=0}^{n} q_i c_i &\ge \sum_{i=0}^{n} q_i' c_i - \sum_{i=0}^{n} q_i c_i = \sum_{i=0}^{n} u_i c_i \\ &= \sum_{i=0}^{k} u_i c_i + \sum_{i=k+1}^{n} u_i c_i \\ &\ge \sum_{i=0}^{k} u_i c_k + \sum_{i=k+1}^{n} u_i c_k = c_k \sum_{i=0}^{n} u_i = 0. \end{aligned} \tag{A20}$$

The other two parts can be proved in the same way. □

Proof of Theorem 1. We will use the first part of Lemma 3 to prove that $\mathbb{E}[a_1/a_s \mid a_s \ge 1] \le \mathbb{E}[a_1'/a_s' \mid a_s' \ge 1]$. Remember that the original system (a_1, a_2) is defined on $(\mathbb{Z}^*)^2$ with $0 \le a_1 \le A_1$, $0 \le a_2 \le A_2$, and $a_1 + a_2 \le S_T$. In the new system, the range is larger: $0 \le a_1' \le A_1 \bar{K}_1/\bar{K}_2$, $0 \le a_2' \le A_2$, and $a_1' + a_2' \le S_T$.

Define

$$\mathbb{P}(x, \cdot) = \sum_{y=0}^{\min(A_2, S_T - x)} \mathbb{P}(x, y), \tag{A21}$$

$$\mathbb{P}'(x, \cdot) = \sum_{y=0}^{\min(A_2, S_T - x)} \mathbb{P}'(x, y). \tag{A22}$$

For $i = 1, \ldots, \min(A_1 \bar{K}_1/\bar{K}_2, S_T)$, set

$$q_i = \frac{\mathbb{P}(i, \cdot)}{1 - \mathbb{P}(0,0)} \quad \text{and} \quad q_i' = \frac{\mathbb{P}'(i, \cdot)}{1 - \mathbb{P}'(0,0)}. \tag{A23}$$

If there exists $i > \min(A_1, S_T)$, stipulate that $q_i = 0$. Set

$$q_0 = \frac{\mathbb{P}(0, \cdot)/\mathbb{P}(0,0)}{1 - \mathbb{P}(0,0)} \quad \text{and} \quad q_0' = \frac{\mathbb{P}'(0, \cdot)/\mathbb{P}'(0,0)}{1 - \mathbb{P}'(0,0)}. \tag{A24}$$

For $i = 1, \ldots, \min(A_1 \bar{K}_1/\bar{K}_2, S_T)$, set

$$c_i = \mathbb{E}[a_1/a_s | a_1 = i] \quad \text{and} \quad c_i' = \mathbb{E}[a_1'/a_s' | a_1' = i]. \tag{A25}$$

If there exists $i > \min(A_1, S_T)$, stipulate that $c_i = \mathbb{E}[a_1'/a_s' \mid a_1' = i]$ and set

$$c_0 = \mathbb{E}[a_1/a_s | a_1 = 0, a_2 \ge 1] = 0, \tag{A26}$$

$$c_0' = \mathbb{E}[a_1'/a_s' | a_1' = 0, a_2' \ge 1] = 0. \tag{A27}$$

If the first part of Lemma 3 applies, then we have

$$\begin{aligned}\mathbb{E}[a_1/a_s \mid a_s \ge 1] &= \mathbb{E}[a_1/a_s \mid a_1 = 0, a_2 \ge 1] \frac{\mathbb{P}(0, \cdot) - \mathbb{P}(0,0)}{1 - \mathbb{P}(0,0)} \\ &\quad + \sum_{i=1}^{\min(A_1, S_T)} \mathbb{E}[a_1/a_s | a_1 = i] \frac{\mathbb{P}(i, \cdot)}{1 - \mathbb{P}(0,0)} \\ &= \sum_i q_i c_i \le \sum_i q_i' c_i' \\ &= \mathbb{E}[a_1'/a_s' | a_1' = 0, a_2' \ge 1] \frac{\mathbb{P}'(0, \cdot) - \mathbb{P}'(0,0)}{1 - \mathbb{P}'(0,0)} \\ &\quad + \sum_{i=1}^{\min(A_1 \bar{K}_1/\bar{K}_2, S_T)} \mathbb{E}[a_1'/a_s' | a_1' = i] \frac{\mathbb{P}'(i, \cdot)}{1 - \mathbb{P}'(0,0)} \\ &= \mathbb{E} a_1'/a_s' | a_s' \ge 1] = \frac{A_1 \bar{K}_1}{A_1 \bar{K}_1 + A_2 \bar{K}_2}. \end{aligned} \tag{A28}$$

To apply the first part of Lemma 3, we need to prove that (i) $c_i = c_i'$, (ii) $q_{i+1} q_i' \le q_i q_{i+1}'$, and (iii) c_i (also c_i') is non-decreasing with i.

(i) Prove $c_x = c_x'$. Since the transition rates along y do not change, we have

$$\begin{aligned}\frac{\mathbb{P}(x, y+1)}{\mathbb{P}(x, y)} &= \frac{r[(x,y) \to (x, y+1)]}{r[(x, y+1) \to (x, y)]} \\ &= \frac{r'[(x,y) \to (x, y+1)]}{r'[(x, y+1) \to (x, y)]} = \frac{\mathbb{P}'(x, y+1)}{\mathbb{P}'(x, y)}, \end{aligned} \tag{A29}$$

which implies

$$\frac{\mathbb{P}(x, y)}{\mathbb{P}(x, \cdot)} = \frac{\mathbb{P}'(x, y)}{\mathbb{P}'(x, \cdot)}. \tag{A30}$$

Thus, for $x \ge 1$,

$$\begin{aligned} c_x &= \sum_{y=0}^{\min\{A_2, S_T - x\}} \frac{\mathbb{P}(x, y)}{\mathbb{P}(x, \cdot)} \cdot \frac{x}{x+y} \\ &= \sum_{y=0}^{\min\{A_2, S_T - x\}} \frac{\mathbb{P}'(x, y)}{\mathbb{P}'(x, \cdot)} \cdot \frac{x}{x+y} = c_x'. \end{aligned} \tag{A31}$$

When $x = 0$, we have $c_0 = \mathbb{E}[a_1/a_s | a_1 = 0, a_2 \ge 1] = \mathbb{E}[a_1'/a_s' | a_1' = 0, a_2' \ge 1] = c_0' = 0$.

(ii) Prove $q_{x+1} q_x' \le q_x q_{x+1}'$. Both systems satisfy detailed balance so that the ratio of stationary probabilities $\mathbb{P}(x, y)$ is the inverse of the ratio of transition rates $r[(x, y) \to (x+1, y)]$,

$$\begin{aligned}\frac{\mathbb{P}(x+1, y)}{\mathbb{P}(x, y)} &= \frac{r[(x,y) \to (x+1, y)]}{r[(x+1, y) \to (x, y)]} \\ &= \frac{(A_1 - x)(S_T - x - y)}{x+1} \bar{K}_1 \\ &\le \frac{(A_1 \bar{K}_1/\bar{K}_2 - x)(S_T - x - y)}{x+1} \bar{K}_2 \\ &= \frac{r'[(x,y) \to (x+1, y)]}{r'[(x+1, y) \to (x, y)]} \\ &= \frac{\mathbb{P}'(x+1, y)}{\mathbb{P}'(x, y)}. \end{aligned} \tag{A32}$$

With $\mathbb{P}(x,\cdot)/\mathbb{P}(x,0) = \mathbb{P}'(x,\cdot)/\mathbb{P}'(x,0)$, we have

$$\begin{aligned}\frac{q_{x+1}}{q_x} &= \frac{\mathbb{P}(x+1,\cdot)/[1-\mathbb{P}(0,0)]}{\mathbb{P}(x,\cdot)/[1-\mathbb{P}(0,0)]}\\ &= \frac{\mathbb{P}(x+1,\cdot)/\mathbb{P}(x+1,0)}{\mathbb{P}(x,\cdot)/\mathbb{P}(x,0)}\cdot\frac{\mathbb{P}(x+1,0)}{\mathbb{P}(x,0)}\\ &= \frac{\mathbb{P}'(x+1,\cdot)/\mathbb{P}'(x+1,0)}{\mathbb{P}'(x,\cdot)/\mathbb{P}'(x,0)}\cdot\frac{\mathbb{P}(x+1,0)}{\mathbb{P}(x,0)}\\ &\le \frac{\mathbb{P}'(x+1,\cdot)/\mathbb{P}'(x+1,0)}{\mathbb{P}'(x,\cdot)/\mathbb{P}'(x,0)}\cdot\frac{\mathbb{P}'(x+1,0)}{\mathbb{P}'(x,0)}\\ &= \frac{\mathbb{P}'(x+1,\cdot)/[1-\mathbb{P}'(0,0)]}{\mathbb{P}'(x,\cdot)/[1-\mathbb{P}'(0,0)]} = \frac{q'_{x+1}}{q'_x}.\end{aligned} \tag{A33}$$

If $q_x = 0$, then $q_{x+1} = 0$ and $q_{x+1}q'_x = q_x q'_{x+1} = 0$. In addition,

$$\begin{aligned}\frac{q_1}{q_0} &= \frac{\mathbb{P}(1,\cdot)/[1-\mathbb{P}(0,0)]}{[\mathbb{P}(0,\cdot)-\mathbb{P}(0,0)]/[1-\mathbb{P}(0,0)]}\\ &= \frac{\mathbb{P}(1,\cdot)/\mathbb{P}(1,0)}{\mathbb{P}(0,\cdot)/\mathbb{P}(0,0)-1}\cdot\frac{\mathbb{P}(1,0)}{\mathbb{P}(0,0)}\\ &\le \frac{\mathbb{P}'(1,\cdot)/\mathbb{P}'(1,0)}{\mathbb{P}'(0,\cdot)/\mathbb{P}'(0,0)-1}\cdot\frac{\mathbb{P}'(1,0)}{\mathbb{P}'(0,0)}\\ &= \frac{\mathbb{P}'(1,\cdot)/[1-\mathbb{P}'(0,0)]}{[\mathbb{P}'(0,\cdot)-\mathbb{P}'(0,0)]/[1-\mathbb{P}'(0,0)]} = \frac{q'_1}{q'_0}.\end{aligned} \tag{A34}$$

(iii) Prove $c'_x \le c'_{x+1}$. For fixed $x \ge 1$ and $i = 0, 1, \ldots,$ min $(A_2, S_T - x)$, set

$$r_i = \mathbb{P}'(x,i)/\mathbb{P}'(x,\cdot), \quad r'_i = \mathbb{P}'(x+1,i)/\mathbb{P}'(x+1,\cdot),$$

$$d_i = x/(x+i), \quad d'_i = (x+1)/(x+1+i).$$

If $A_2 \ge S_T - x$, stipulate $r'_{S_T-x} = \mathbb{P}'(x+1, S_T-x)/\mathbb{P}'(x+1,\cdot) = 0$.

If the third part of Lemma 3 applies, then for $x \ge 1$,

$$\begin{aligned}c'_x &= \mathbb{E}[a'_1/a'_s|a'_1 = x] = \sum_{i=0}^{\min(A_2,S_T-x)} r_i d_i\\ &\le \sum_{i=0}^{\min(A_2,S_T-x)} r_{i'} d_{i'} = \mathbb{E}[a'_1/a'_s|a'_1 = x+1] = c'_{x+1}.\end{aligned} \tag{A35}$$

In addition, $c'_1 = \mathbb{E}[a'_1/a'_s \,|\, a'_1 = 1] \ge \mathbb{E}[a'_1/a'_s \,|\, a'_1 = 0, a'_2 \ge 1] = c'_0 = 0$.

To apply the third part of Lemma 3, we can verify that $d_i \ge d_{i+1}$, $d'_i \ge d'_{i+1}$, $d_i \le d'_i$. To prove $r_{i+1}r'_i \ge r_i r'_{i+1}$, note that

$$\begin{aligned}\frac{r_{y+1}}{r_y} &= \frac{\mathbb{P}'(x,y+1)/\mathbb{P}'(x,\cdot)}{\mathbb{P}'(x,y)/\mathbb{P}'(x,\cdot)} = \frac{(A_2-y)(S_T-x-y)}{y+1}\bar{K}_2\\ &\ge \frac{(A_2-y)(S_T-x-y-1)}{y+1}\bar{K}_2\\ &= \frac{\mathbb{P}'(x+1,y+1)/\mathbb{P}'(x+1,\cdot)}{\mathbb{P}'(x+1,y)/\mathbb{P}'(x+1,\cdot)} = \frac{r'_{y+1}}{r'_y}.\end{aligned} \tag{A36}$$

□

Proof of Theorem 2. Consider a mixture of A_1 molecules of aptamer A''_1 with association coefficient $\bar{K}_2$, A_2 molecules of aptamer A''_2 with association coefficient $\bar{K}_2$, and S_T molecules of the target. In this mixture, all aptamers have the same association coefficient. Due to symmetry, we apparently have $\mathbb{E}[a''_1/a''_s \,|\, a''_s \ge 1] = A_1/(A_1+A_2)$. Then, we only need to prove $\mathbb{E}[a_1/a_s|a_s \ge 1] \ge \mathbb{E}[a''_1/a''_s \,|\, a''_s \ge 1]$.

We define q_i, q'_i, c_i, c'_i as in the Proof of Theorem 1 and apply the second part of Lemma 3. The only difference is that

$$\begin{aligned}\frac{\mathbb{P}(x+1,y)}{\mathbb{P}(x,y)} &= \frac{(A_1-x)(S_T-x-y)}{x+1}\bar{K}_1\\ &\ge \frac{(A_1-x)(S_T-x-y)}{x+1}\bar{K}_2 = \frac{\mathbb{P}''(x+1,y)}{\mathbb{P}''(x,y)}\end{aligned} \tag{A37}$$

so that $q_{x+1}q'_x \ge q_x q'_{x+1}$. Then, by the second part of Lemma 3,

$$\begin{aligned}\mathbb{E}[a_1/a_s|a_s \ge 1] &= \sum_i q_i c_i\\ &\ge \sum_i q'_i c'_i = \mathbb{E}[a''_1/a''_s|a''_s \ge 1].\end{aligned} \tag{A38}$$

□

Following the Proof of Theorem 1, we can also prove another result.

Proposition 1. If $A_1\bar{K}_1/\bar{K}_2$ is an integer and $A_1 > S_T$, then

$$\mathbb{E}[a_1/a_s|a_s \ge 1] \ge \frac{A_1\bar{K}_1}{A_1\bar{K}_1 + A_2\bar{K}_2}\cdot\left(1 - \frac{S_T^2}{A_1 - S_T}\right). \tag{A39}$$

This provides a better explanation of the results in Sec. IV A: *$A_i \gg S_T^2$ for each i is enough for $\mathbb{E}[a_1/a_s \,|\, a_s \ge 1]$ to reach its upper bound.*

Proof. When $A_1 > S_T$, c_i, c'_i, q_i, q'_i as in the Proof of Theorem 1 are all defined for $i = 0, 1, \ldots, S_T$. We have $q_0 \ge q'_0$; otherwise, since $q_{i+1}/q_i \le q'_{i+1}/q'_i$, we have $q_i < q'_i$ for all i, which contradicts $\sum_i q_i = \sum_i q'_i = 1$.

For any $i \le S_T$, we have

$$\begin{aligned}\frac{q_i}{q'_i} &= \frac{q_0\prod_{j=0}^{i-1}(q_{j+1}/q_j)}{q'_0\prod_{j=0}^{i-1}(q'_{j+1}/q'_j)} \ge \prod_{j=0}^{i-1}\frac{q_{j+1}/q_j}{q'_{j+1}/q'_j}\\ &= \prod_{j=0}^{i-1}\frac{A_1\bar{K}_1 - j\bar{K}_1}{A_1\bar{K}_1 - j\bar{K}_2} = \prod_{j=0}^{i-1}\left(1 - \frac{j\bar{K}_1 - j\bar{K}_2}{A_1\bar{K}_1 - j\bar{K}_2}\right)\\ &\ge \prod_{j=0}^{i-1}\left(1 - \frac{S_T\bar{K}_1}{A_1\bar{K}_1 - S_T\bar{K}_1}\right) \ge \left(1 - \frac{S_T}{A_1 - S_T}\right)^{S_T}\\ &\ge 1 - \frac{S_T^2}{A_1 - S_T},\end{aligned} \tag{A40}$$

where the last inequality is from the Taylor expansion with Lagrange remainder for $(1-x)^n$ at $x = 0$. Then,

$$\frac{\mathbb{E}[a_1/a_s \,|\, a_s \ge 1]}{\mathbb{E}[a'_1/a'_s \,|\, a'_s \ge 1]} = \frac{\sum_i c_i q_i}{\sum_i c'_i q'_i} \ge 1 - \frac{S_T^2}{A_1 - S_T}. \tag{A41}$$

□

However, Proposition 1 is rather loose, and $A_i \gg S_T^2$ is not necessary for $\mathbb{E}[a_1/a_s \,|\, a_s \ge 1]$ to be close to its upper bound.

6. Proof of Theorem 3

For a ratio $r \in [0,1]$, define $f(r) = r\tilde{K}_1/[r\tilde{K}_1 + (1-r)\tilde{K}_2]$. If the current fraction of aptamers that are A_1 is r_0, then after one round of policy 1 or policy 2, the expected fraction of A_1 aptamers becomes $f(r_0)$. Note that $f(r_0)$ is simply the maximum expected fraction of A_1 after one round of SELEX that was initiated with the ratio $A_1/(A_1+A_2)$. Denote the kth iteration of f by $f^{(k)}(r)$, which equals $r\tilde{K}_1^k/[r\tilde{K}_1^k + (1-r)\tilde{K}_2^k]$. We can verify that $f^{(k)}(r)$ is strictly increasing and concave in r. We now inductively prove that if the A_1 proportion after round $N-k$ is r, then after round N, the maximal expected A_1 proportion is $f^{(k)}(r)$.

Assume that $a_1/a_s = r_0^{(N-1)}$ after round $N-1$. For round N, policies 1 and 2 both reach the upper bound $\mathbb{E}[a_1/a_s] = f(r_0^{(N-1)})$. Therefore, the optimal policy for the last round is either policy 1 or policy 2. Assume that this statement is valid for $k = K$. For $k = K+1$, assume $a_1/a_s = r_0^{(N-K-1)}$ after round $N-K-1$. If we apply policy 1, then after round $N-K$, $a_1/a_s = f(r_0^{(N-K-1)})$. After round N, the optimal policy produces $\mathbb{E}[a_1/a_s] = f^{(K+1)}(r_0^{(N-K-1)})$. Assume we apply another policy for round $N-K$ and the distribution of a_1/a_s after round $N-K$ is $\mathbb{P}(a_1/a_s = r_i) = q_i$, where $i = 1,\ldots,L$ and $\sum_{i=1}^{L} q_i r_i = r_0'$. After round N, the optimal policy produces $\mathbb{E}[a_1/a_s] = \sum_{i=1}^{L} f^{(K)}(r_i)$. We have

$$\begin{aligned}\sum_{i=1}^{L} q_i f^{(K)}(r_i) &\le f^{(K)}\left(\sum_{i=1}^{L} q_i r_i\right)\\ &= f^{(K)}(r_0')\\ &\le f^{(K)}\left(f(r_0^{(N-K-1)})\right)\\ &= f^{(K+1)}(r_0^{(N-K-1)}).\end{aligned} \tag{A42}$$

Here, the first relationship arises from Jensen's inequality, and policies 2 or 4 cannot make it an equality. The second inequality arises from $r_0' \le f(r_0^{(N-K-1)})$, and policy 3 cannot make it an equality. Therefore, we have proved the statement for $k = K+1$, and policy 1 is the only optimal policy for round $N-K$.

By induction, starting with $A_1/(A_1+A_2) = r_0^{(0)}$, the maximal proportion of aptamer A_1 after N rounds of SELEX is $f^{(N)}(r_0^{(0)}) = A_1\tilde{K}_1^N/(A_1\tilde{K}_1^N + A_2\tilde{K}_2^N)$. Since $\tilde{K}_1 > \tilde{K}_2$, this means that $1 - \mathbb{E}[a_1/a_s]$ converges to 0 exponentially fast, as the name SELEX (Systematic Evolution of Ligands by EXponential enrichment) implies. Policy 1 is the optimal policy for the first $N-1$ rounds. For round N, policy 1 and policy 2 are both optimal.

REFERENCES

[1] J. K. Osbourn, J. C. Earnshaw, K. S. Johnson, M. Parmentier, V. Timmermans, and J. McCafferty, "Directed selection of MIP-1α neutralizing CCR5 antibodies from a phage display human antibody library," Nat. Biotechnol. **16**, 778–781 (1998).

[2] A. Pegu, Z. Y. Yang, J. C. Boyington, L. Wu, S. Y. Ko, S. D. Schmidt, K. McKee, W. P. Kong, W. Shi, X. Chen, J. P. Todd, N. L. Letvin, J. Huang, M. C. Nason, J. A. Hoxie, P. D. Kwong, M. Connors, S. S. Rao, J. R. Mascola, and G. J. Nabel, "Neutralizing antibodies to HIV-1 envelope protect more effectively in vivo than those to the CD4 receptor," Sci. Transl. Med. **6**, 243ra88 (2014).

[3] L. Harvey, B. Arnold, and M. Paul, *Molecular Cell Biology* (W. H. Freeman, 2004).

[4] K. Qian, S. L. Morris-Natschke, and K.-H. Lee, "HIV entry inhibitors and their potential in HIV therapy," Med. Res. Rev. **29**, 369–393 (2009).

[5] J. P. Moore and R. W. Doms, "The entry of entry inhibitors: A fusion of science and medicine," Proc. Natl. Acad. Sci. U. S. A. **100**, 10598–10602 (2003).

[6] S. Qiu, H. Yi, J. Hu, Z. Cao, Y. Wu, and W. Li, "The binding mode of fusion inhibitor T20 onto HIV-1 gp41 and relevant T20-resistant mechanisms explored by computational study," Curr. HIV Res. **10**, 182–194 (2012).

[7] G. Neumann, K. Fujii, Y. Kino, and Y. Kawaoka, "An improved reverse genetics system for influenza A virus generation and its implications for vaccine production," Proc. Natl. Acad. Sci. U. S. A. **102**, 16825–16829 (2005).

[8] C. Gerdil, "The annual production cycle for influenza vaccine," Vaccine **21**, 1776–1779 (2003).

[9] J. A. Tree, C. Richardson, A. R. Fooks, J. C. Clegg, and D. Looby, "Comparison of large-scale mammalian cell culture systems with egg culture for the production of influenza virus A vaccine strains," Vaccine **19**, 3444 (2001).

[10] S. Meyer, J. P. Maufort, J. Nie, R. Stewart, B. E. McIntosh, L. R. Conti, K. M. Ahmad, H. T. Soh, and J. A. Thomson, "Development of an efficient targeted cell-SELEX procedure for DNA aptamer reagents," PLoS ONE **8**, e71798 (2013).

[11] J. Wang, J. F. Rudzinski, Q. Gong, H. T. Soh, and P. J. Atzberger, "Influence of target concentration and background binding on *in vitro* selection of affinity reagents," PLoS ONE **7**, e43940 (2012).

[12] H. A. Levine, Y.-J. Seo, and M. Nilsen-Hamilton, "A discrete dynamical system arising in molecular biology," Discrete Contin. Dyn. Syst. B **17**, 2091–2151 (2012).

[13] N. Komarova and A. Kuznetsov, "Inside the black box: What makes SELEX better?," Molecules **24**(19), 3598 (2019).

[14] F. Spill, Z. B. Weinstein, A. Weinstein, N. Ho, D. Desai, and M. H. Zaman, "Controlling uncertainty in aptamer selection," Proc. Natl. Acad. Sci. **113**(43), 12076–12081 (2016).

[15] Y.-J. Seo, S. Chen, M. Nilsen-Hamilton, and H. A. Levine, "A mathematical analysis of multiple-target SELEX," Bull. Math. Biol. **72**(7), 1623–1665 (2010).

[16] Y.-J. Seo, M. Nilsen-Hamilton, and H. A. Levine, "A computational study of alternate SELEX," Bull. Math. Biol. **76**(7), 1455–1521 (2014).

[17] T. Aita, K. Nishigaki, and Y. Husimi, "Theoretical consideration of selective enrichment in in vitro selection: Optimal concentration of target molecules," Math. Biosci. **240**(2), 201–211 (2012).

[18] D.-Q. Jiang, M. Qian, and M.-P. Qian, *Mathematical Theory of Nonequilibrium Steady States: On the Frontier of Probability and Dynamical Systems* (Springer Science & Business Media, 2004).

[19] Y. Wang and H. Qian, "Mathematical representation of Clausius' and Kelvin's statements of the second law and irreversibility," J. Stat. Phys. **179**, 808–837 (2020).

[20] J. Atherton, B. Nathan, B. Brown, N. Ogawa, S. M. Davidson, M. B. Eisen, M. D. Biggin, and P. Bickel, "A model for sequential evolution of ligands by exponential enrichment (SELEX) data," Ann. Appl. Stat. **6**(3), 928–949 (2012).

[21] D. H. De Jong, L. V. Schäfer, A. H. De Vries, S. J. Marrink, H. J. C. Berendsen, and H. Grubmüller, "Determining equilibrium constants for dimerization reactions from molecular dynamics simulations," J. Comput. Chem. **32**(9), 1919–1928 (2011).

[22] H. A. Levine and M. Nilsen-Hamilton, "A mathematical analysis of SELEX," Comput. Biol. Chem. **31**(1), 11–35 (2007).

[23] Although in practice, it is not easy to independently control A_1.

[24] J. J. Hopfield, "Kinetic proofreading: A new mechanism for reducing errors in biosynthetic processes requiring high specificity," Proc. Natl. Acad. Sci. **71**(10), 4135–4139 (1974).

[25] T. G. Kurtz, "Limit theorems for sequences of jump Markov processes approximating ordinary differential processes," J. Appl. Probab. **8**(2), 344–356 (1971).

[26] D. F. Anderson and T. G. Kurtz, "Continuous time Markov chain models for chemical reaction networks," in *Design and Analysis of Biomolecular Circuits* (Springer, 2011), pp. 3–42.

[27] P. Thomas, C. Fleck, R. Grima, and N. Popović, "System size expansion using Feynman rules and diagrams," J. Phys. A: Math. Theor. **47**(45), 455007 (2014).

[28] D. A. Kessler and N. M. Shnerb, "Extinction rates for fluctuation-induced metastabilities: A realspace WKB approach," J. Stat. Phys. **127**, 861–886 (2007).

[29]C.-K. Chen, "Complex SELEX against target mixture: Stochastic computer model, simulation, and analysis," Comput. Methods Programs Biomed. **87**(3), 189–200 (2007).
[30]B. A. Mistry and T. Chou, "Nonspecific probe binding and automatic gating in flow cytometry and fluorescence activated cell sorting (FACS)," Math. Biosci. Eng. **16**, 4477–4490 (2019).
[31]M. Georgieva, C. O. Buckee, and M. Lipsitch, "Models of immune selection for multi-locus antigenic diversity of pathogens," Nat. Rev. Immunol. **19**(1), 55–62 (2019).
[32]L. Ma, D. Lai, T. Liu, W. Cheng, and L. Guo, "Cancer stem-like cells can be isolated with drug selection in human ovarian cancer cell line SKOV3," Acta Biochim. Biophys. Sin. **42**(9), 593–602 (2010).
[33]L. Sandegren, "Selection of antibiotic resistance at very low antibiotic concentrations," Upsala J. Med. Sci. **119**(2), 103–107 (2014).
[34]T. Chou and M. R. D'Orsogna, "Coarsening and accelerated equilibration in mass-conserving heterogeneous nucleation," Phys. Rev. E **84**, 011608 (2011).
[35]M. R. D'Orsogna, G. Lakatos, and T. Chou, "Stochastic self-assembly of incommensurate clusters," J. Chem. Phys. **136**(8), 084110 (2012).